Remote Sensing Solutions, Inc.

PROJECT: Operational SFMR-NAWIPS Airborne Processing and Data Distribution Products

NOAA Award No.: NA05OAR4171101

Interim Report – Year 2

Prepared By: Dr. James Carswell

Date: 02/28/2007

1 INTRODUCTION

1.1 SCOPE

This document summarizes the work performed and accomplishments achieved to date in the second year effort of the Joint Hurricane Testbed (JHT) project entitled, "Operational SFMR-NAWIPS Airborne Processing and Data Distribution Products.

1.2 DOCUMENT BREAKDOWN

This document contains three sections. Section 1 contains the introduction. Section 2 reviews the work performed to date during the second year of this effort. Section 3 discusses the work that will be performed prior to the 2007 Hurricane season.

2 SECOND YEAR – WORK PERFORMED

During the first half of the second year effort, the JHT SFMR team focused on analyzing the SFMR observations and retrievals obtained during the 2006 Hurricane season with the objective of identifying and explaining anomalies; identifying and removing the sources of RFI that increased the uncertainty in the SFMR estimates during the 2006 hurricane season; and developing a new precipitation geophysical model function (GMF) for use within the SFMR retrieval process. Below these efforts are summarized. RSS also developed and deployed a real-time GIS and time series display and analysis application that enabled users at NHC and HRD to visualize and interact with the SFMR and flight level data. This application was presented at the NHC conference. If more information is desired on this particular application, please contact Jim Carswell at carswell@rmss.us.

2.1 2006 Hurricane Season - SFMR Anomalies

The JHT team reviewed the SFMR measurements and retrievals from the 2006 hurricane season. Anomalies were found in the SFMR retrievals during missions through Hurricane Ernesto on the 29th and 31st of August.

Figures 1 and 3 map the SFMR wind retrievals for the flights on August 29 and 31. The NOAA N42RF aircraft was flown for these missions with the US002 AOC SFMR. The time stamps, shown in green, mark the regions where problems in the SFMR retrievals were discovered. Figures 2 and 4 show the corresponding multiple time series plots of the SFMR retrievals (wind and rain rate). More detailed time series plots will be shown and a quick summary is given below:

- *August 29th mission*: The 10 second averaged SFMR wind retrievals exceeded the storm force threshold but did not reach hurricane force. Five anomalies were noted.
- *August 31st mission*: This was the second landfall mission. The 10 second averaged SFMR wind retrievals exceeded the storm force threshold but

did not reach hurricane force. Five anomalies in the SFMR wind retrievals were observed.

In the subsections to follow, the observed anomalies are presented and their causes explained. The anomalies are believed to be due to either low water depth or caused by limitations in the precipitation model used in the SFMR retrieval process. Recall that in our annual report, we showed that errors in the rain retrieval could translate to errors in the wind retrieval. In the future, the anomalies caused by low water depths can be prevented by augmenting the land mask filter to include areas of shallow bathymetry (less than approximately 30 m). Anomalies caused by errors in the precipitation model are to be addressed as part of the 2nd year JHT SFMR effort which is focused on constructing a new precipitation model.

Before discussing these cases, however, it should be noted that some concern raised by forecasters may have occurred because the high resolution SFMR retrievals, as well as the averaged retrievals, were made available to NHC through RSS' Real-time Display Application. These high resolution measurements exhibit more variance than NHC may be accustomed to seeing. The variance is due to the shorter integration time (one second versus ten or 30 seconds). We calculated the expected standard deviation for these retrievals based on the performance specifications of the AOC SFMR and found the measured standard deviation for the retrievals agreed well with the predictions. In the future, we recommend that the standard product be at least a 10 point or 10 second average to reduce this variance, and we will modify our Real-time Display application accordingly.

2.1.1 Anomalies - 29 August 2006

Six anomalies in the SFMR retrievals were observed during the August 29th mission. Each anomaly is presented below and its causes explained. In the following figures, the 10 second averaged SFMR and flight level winds are plotted as red and purple lines, respectively. The high resolution SFMR wind speed retrievals are plotted as points. The SFMR rain rate retrievals are plotted as a blue line. The collocated water depth estimate (2 minute resolution bathymetry data) is shown as a green line. If not present, the water depth is greater than 100 m.

Figure 5 shows the observed anomaly at approximately 15.975 hours. At this time a rain event occurred. The SFMR wind speed retrieval decreased by more than 10 kts at the beginning of the rain event and increased to approximately 60 kts following the rain event. The flight level winds were relatively flat. We believe that the SFMR wind speed estimates are in error. This wind speed error is due to the current limitations in the SFMR precipitation model. That is, the current precipitation model does not adequately describe the brightness temperature dependence on rain rate. At lower wind speeds (below hurricane force winds) this can cause a convergence problem in the retrieval process. Often, as in this

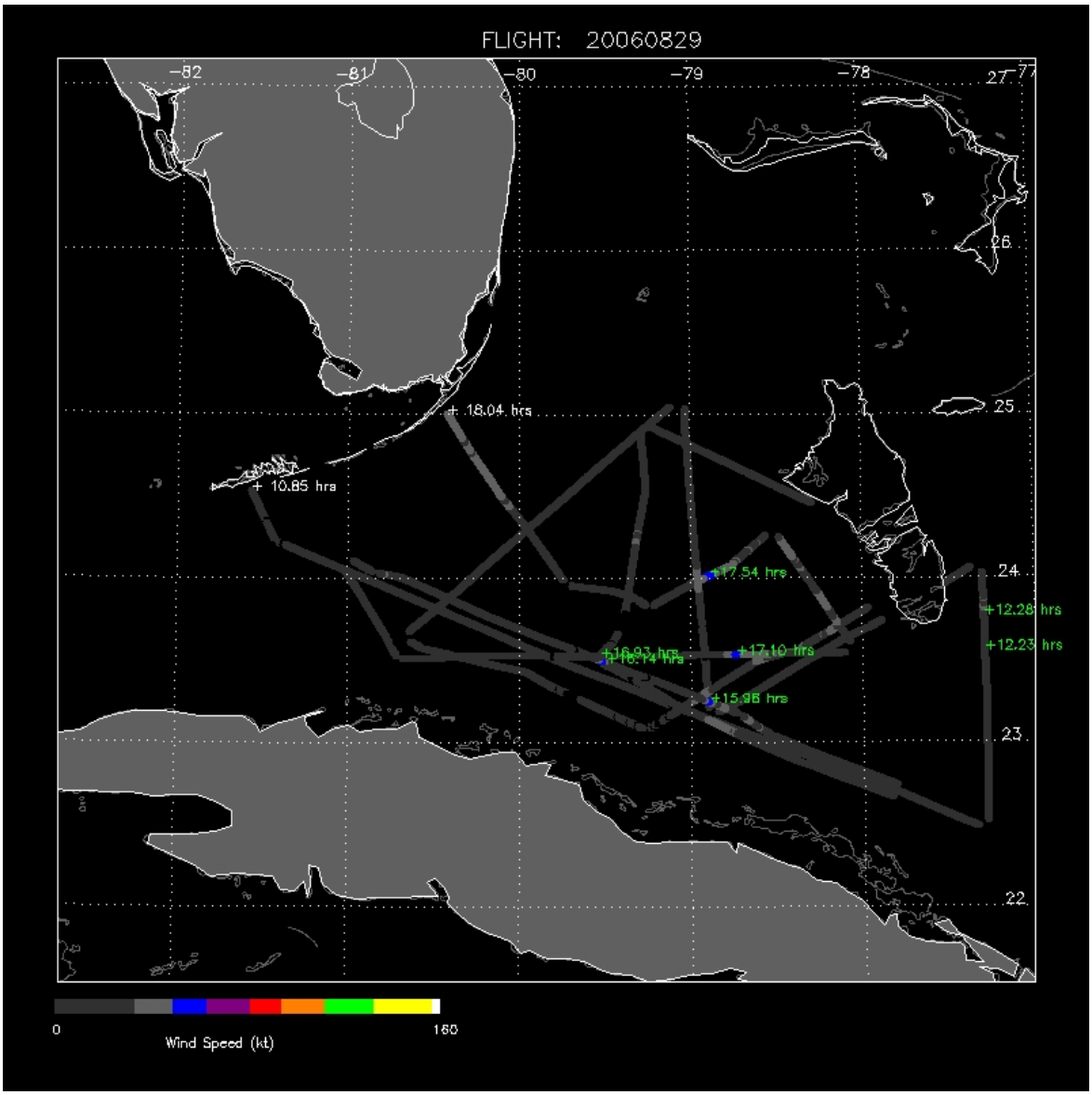

Figure 1: Geolocated SFMR winds estimates from 29 August, 2006.

case, the convergence problem will cause the wind speed retrievals to oscillate. By looking for a dip as well as a rise in the wind speed and comparing them against the flight level wind speeds, these errors can be detected. Likewise, at 16.05 hrs, the SFMR winds also excessively increased during a precipitation event and did not reflect the true surface wind. A similar event to this occurred again at 17.12 hours and at 17.55 hours (Figure 8 and Figure 9) Once the precipitation model has been corrected, we expect that these types of anomalies will not occur.

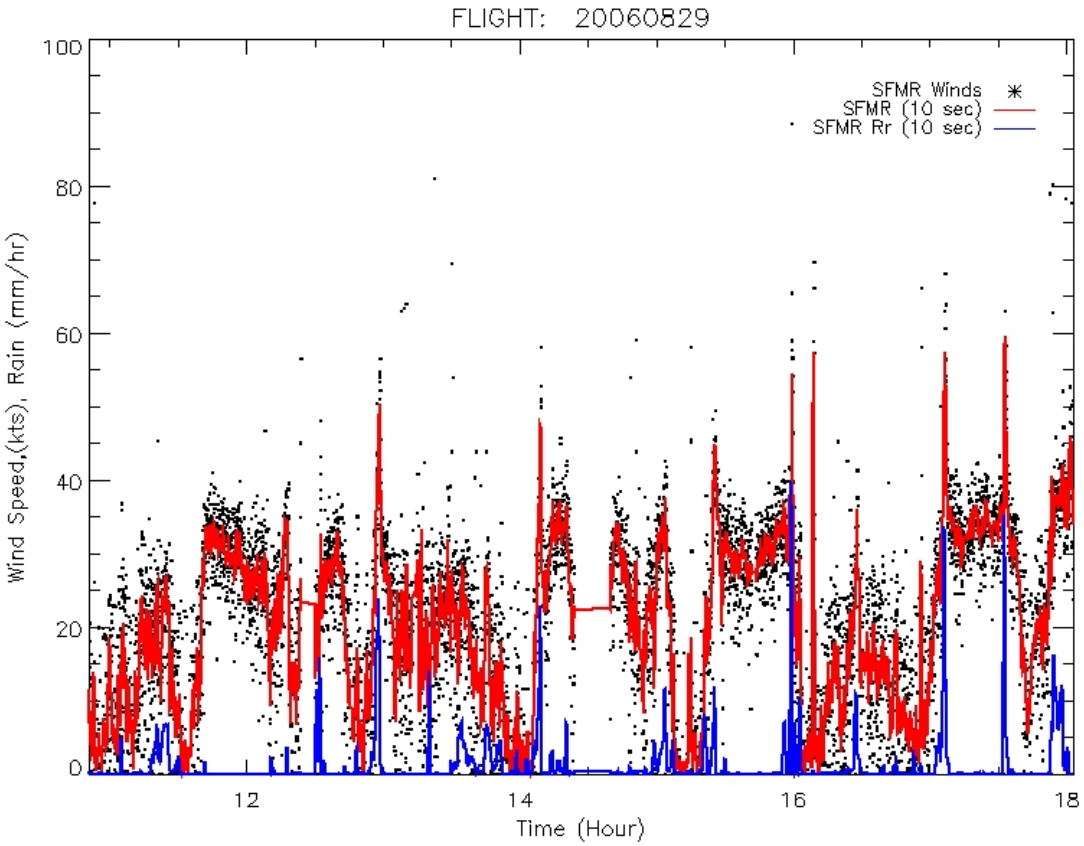

Figure 2: Time series plot of the SFMR wind retrievals (points) and averaged SFMR wind speed and rain rate retrievals (red, blue) acquired on 29 August, 2006.

As mentioned previously, low water depth can also cause an artificial increase in the SFMR wind speed retrievals by causing enhanced wave breaking and thus more foam generation. We believe that this explains the anomalies at 16.15 hrs (figure 8) and 16.94 hrs (figure 9) where the SFMR winds significantly increased as the water depth became shallow (less than 30 m). Note that in Figure 8, the water depth at 16.15 hrs appears to be approx 70 m and then drops to 20 m. The spatial resolution / sampling of the bathymetry data are on the order of 3 km.

The 70 m measurements are more than 1.5 km from the track whereas the 20 m water depth measurements are within less than 500 m. The enhanced SFMR winds at 17.12 hrs may have also been partially attributed to a sharp decrease in the water depth. It is difficult to discern this however since both rain and low water depths occurred at this time.

To illustrate the complexity of bathymetry effects, Figure 10 shows a picture taken from the WP-3D aircraft at 12:14 GMT (12.23 hours). In this image, small land features and the effects of bathymetry can be seen. The shallow water and land features prevent the long wave structure seen in the lower half of the image from propagating to the area in the upper half. Wave breaking events that generate foam are seen in the lower part of the image but are not seen in the

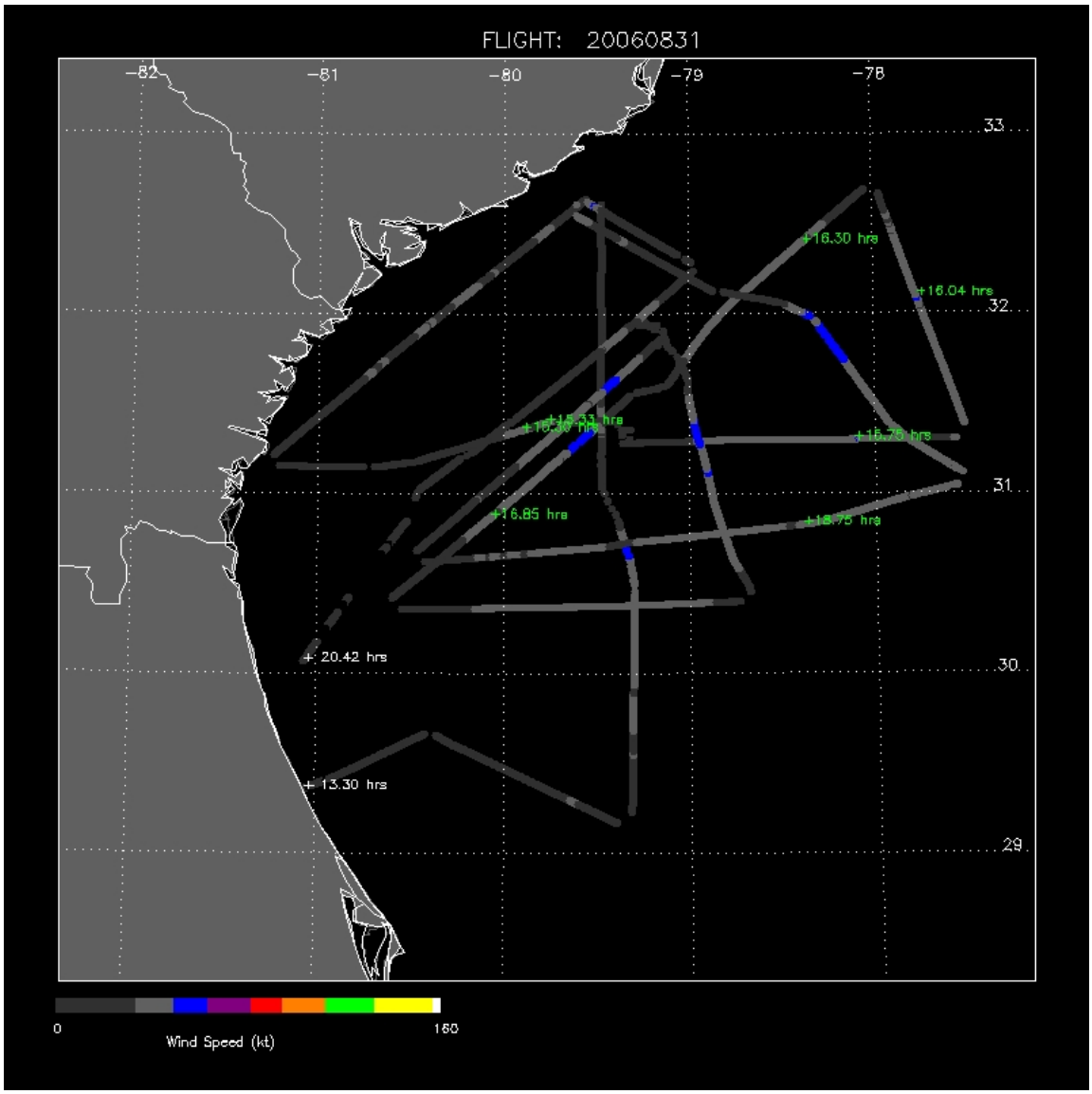

Figure 3: Geolocated SFMR winds estimates from 31 August, 2006

upper half even though the wind is believed to be fairly constant. In such a situation, the SFMR would retrieve different winds in these two areas. Further, the small land features are not detected in our current land mask and may contaminate the brightness temperature measurements, and thus contaminate the SFMR retrievals. Figure 11 presents the SFMR retrievals around the time this picture was taken. At 12.23 hours, the wind appears to increase. It is difficult to discern whether the wind actually increased, land contamination occurred or enhanced wave breaking occurred due to shallow water. Note that the flight level winds do not show a corresponding increase.

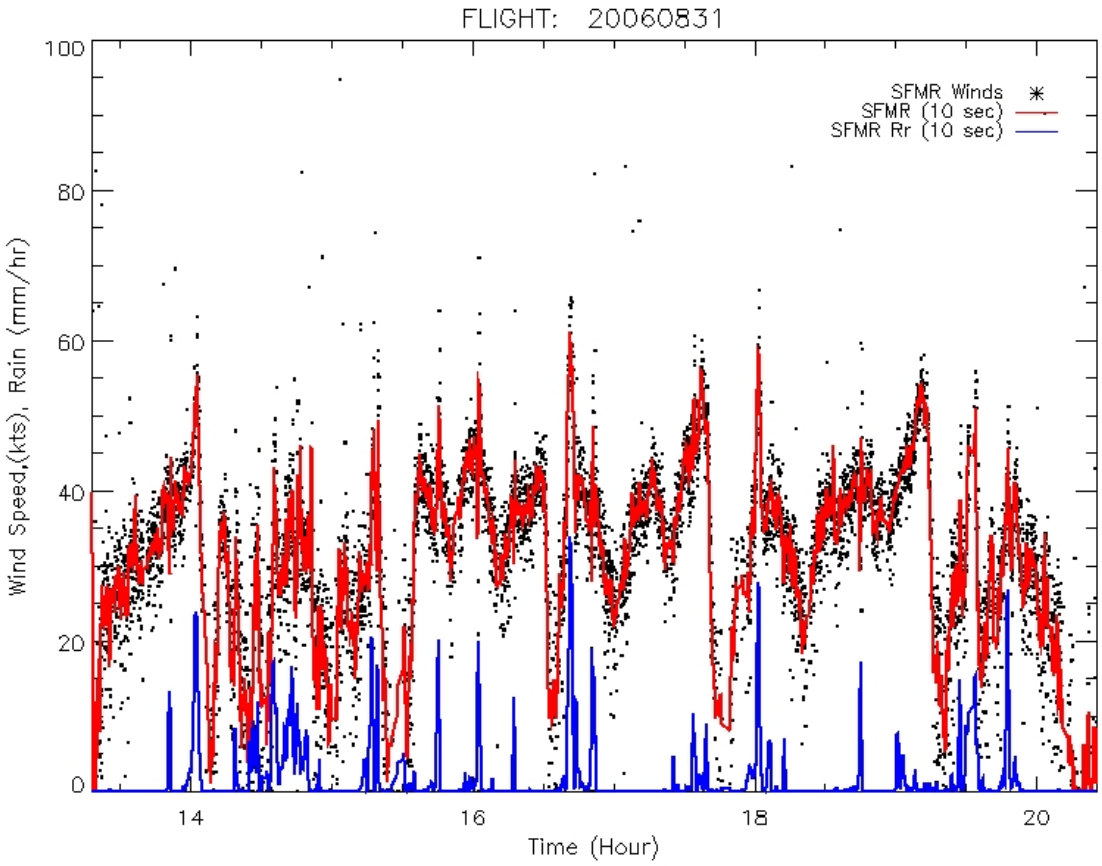

Figure 4: Time series plot of the SFMR wind retrievals (points) and averaged SFMR wind speed and rain rate retrievals (red, blue) acquired on 31 August, 2006.

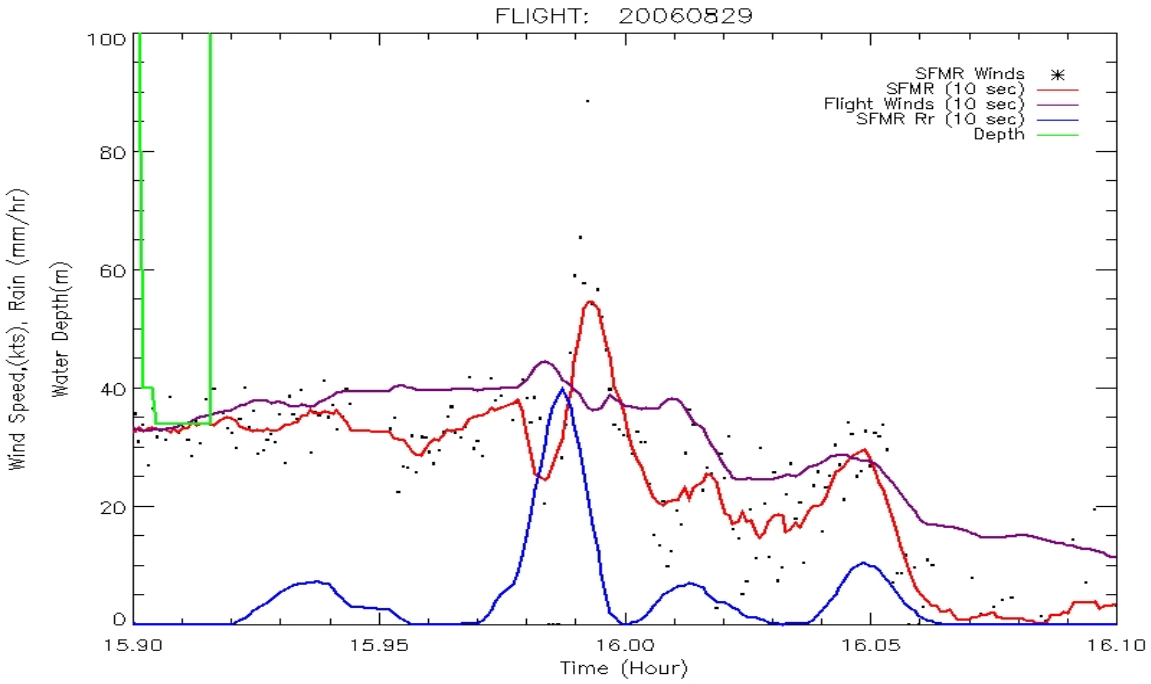

Figure 5: Anomaly in the SFMR wind retrieval is shown at approximately 15.975 hours on 29 August 2006.

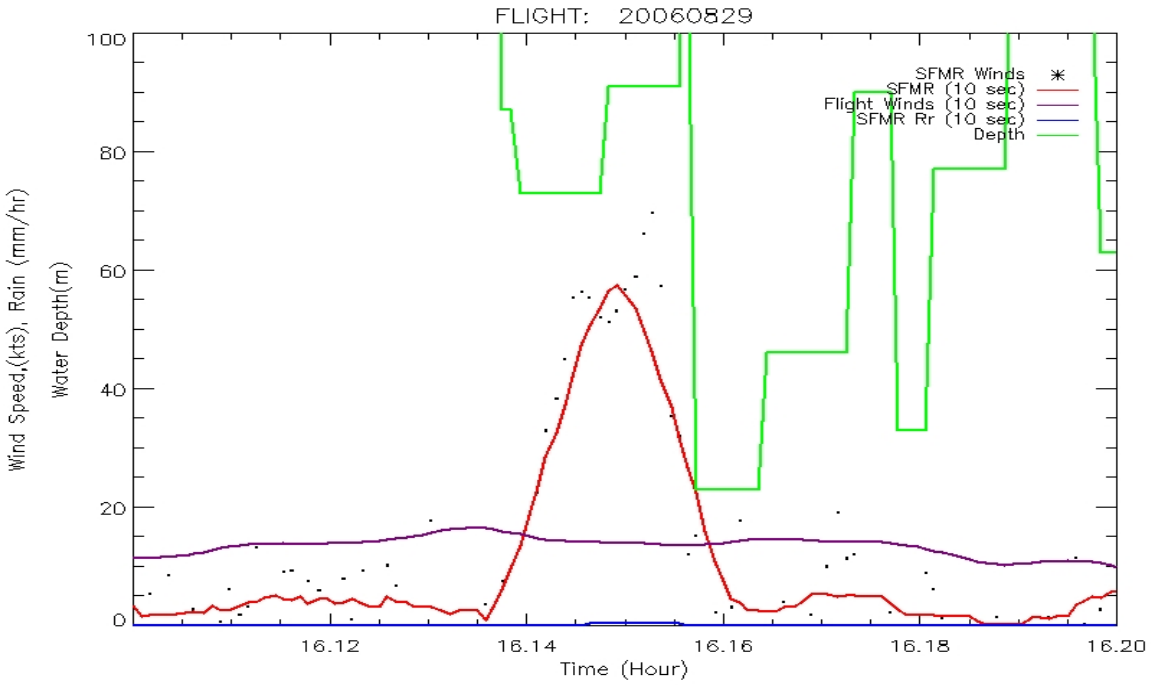

Figure 6: Anomaly in the SFMR wind retrieval is shown at approximately 16.15 hours on 29 August 2006.

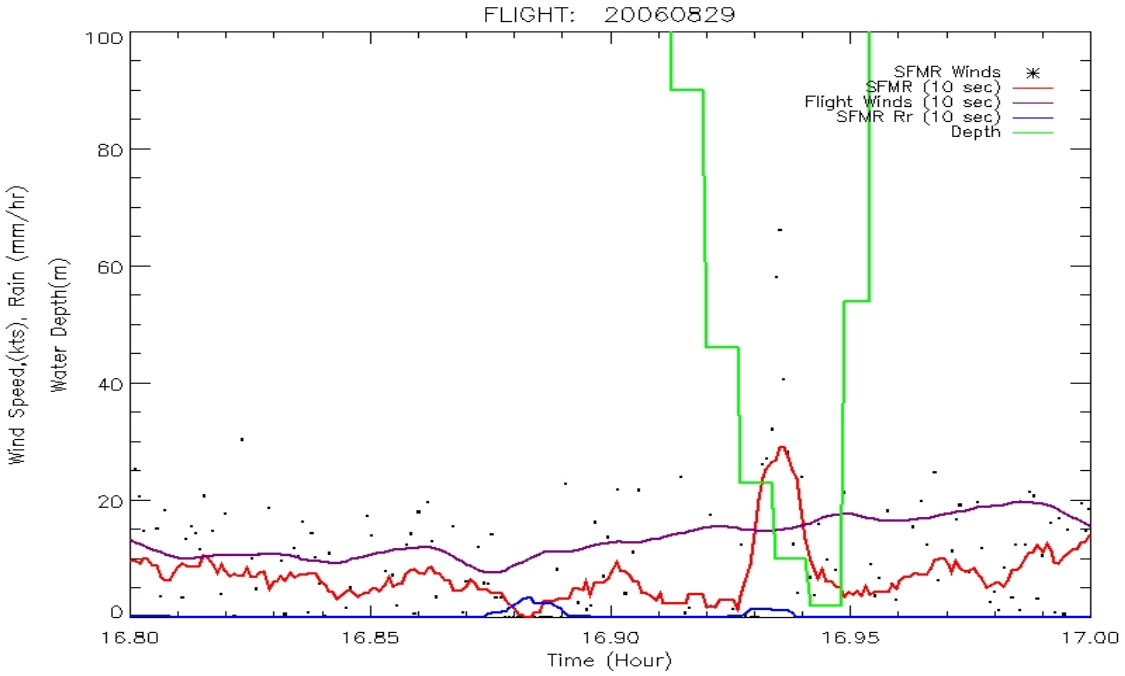

Figure 7: Anomaly in the SFMR wind retrieval is shown at approximately 16.94 hours on 29 August 2006.

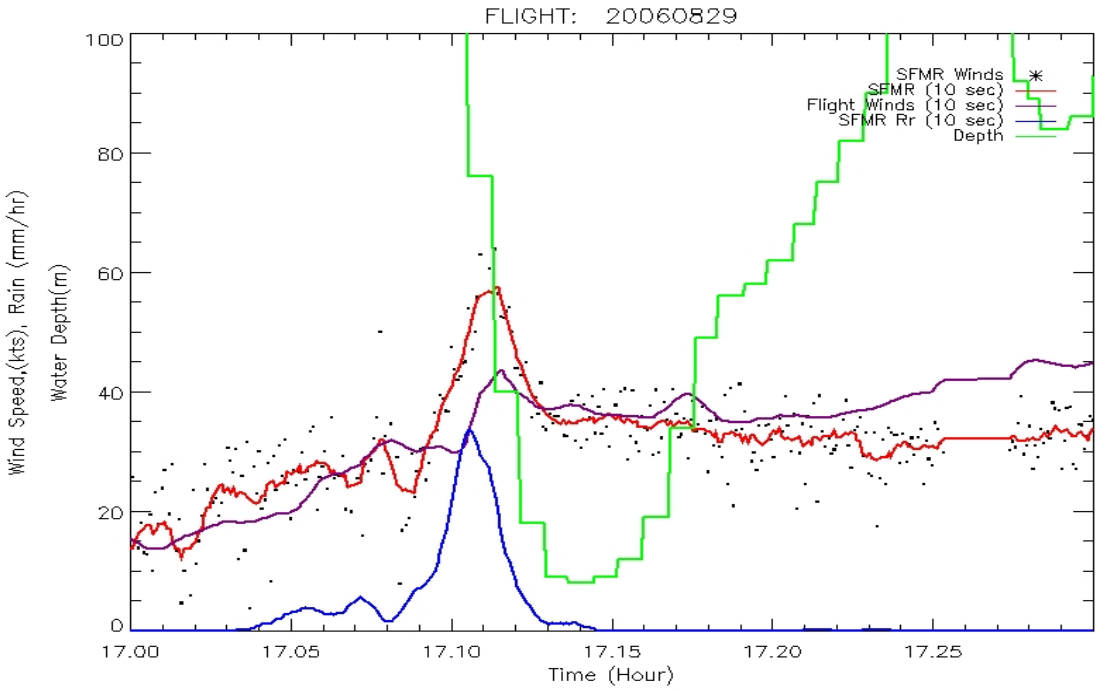

Figure 8: Anomaly in the SFMR wind retrieval is shown at approximately 17.12 hours on 29 August 2006.

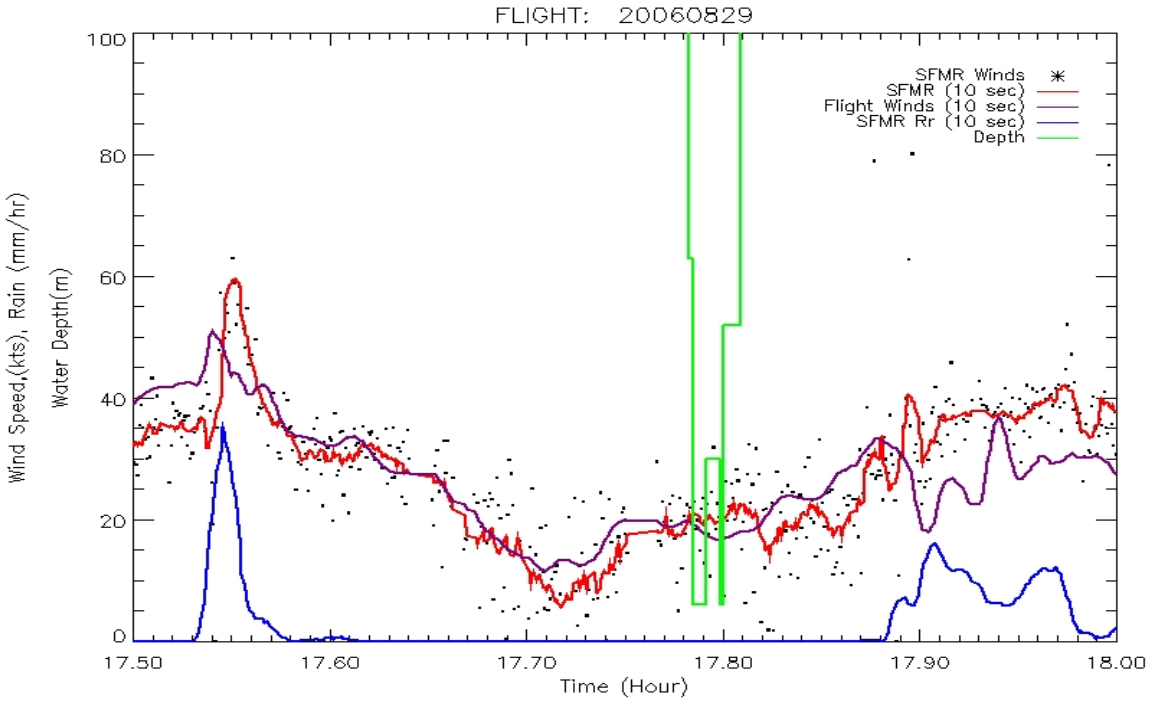

Figure 9: Anomalies in the SFMR wind retrieval are shown at approximately 17.55 and 17.9 hours on 29 August 2006.

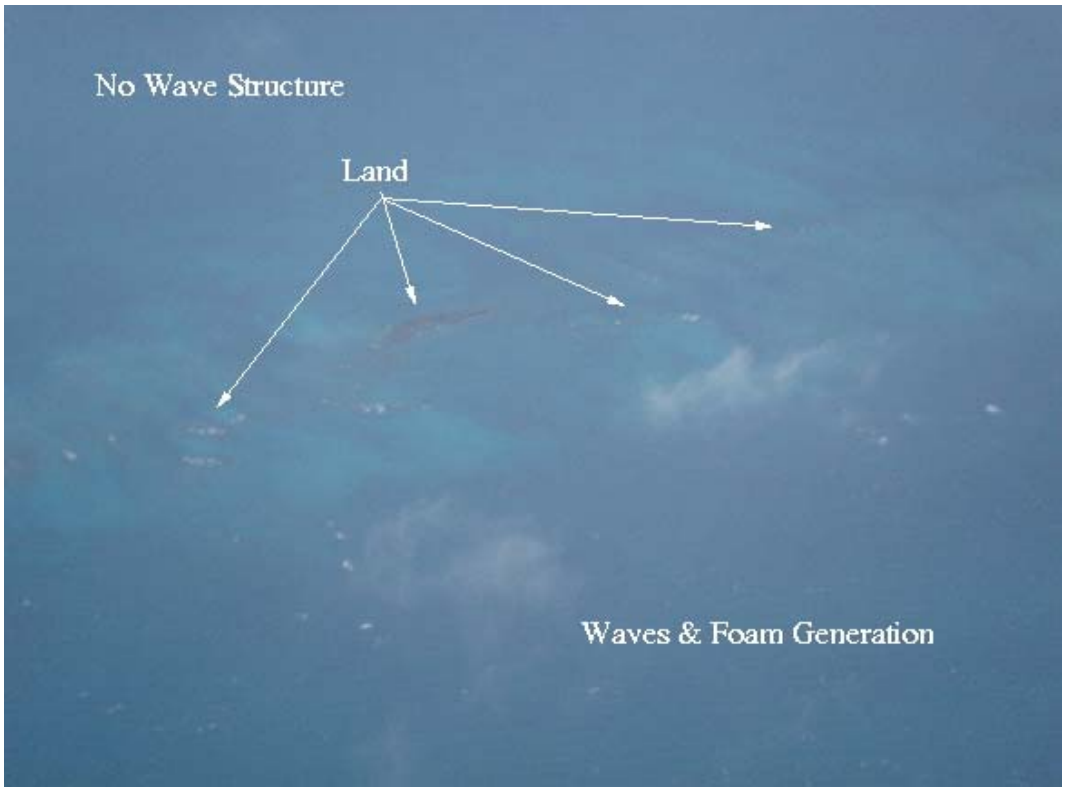

Figure 10: Picture taken from WP-3D aircraft at 12:14 on 29 August, 2006.

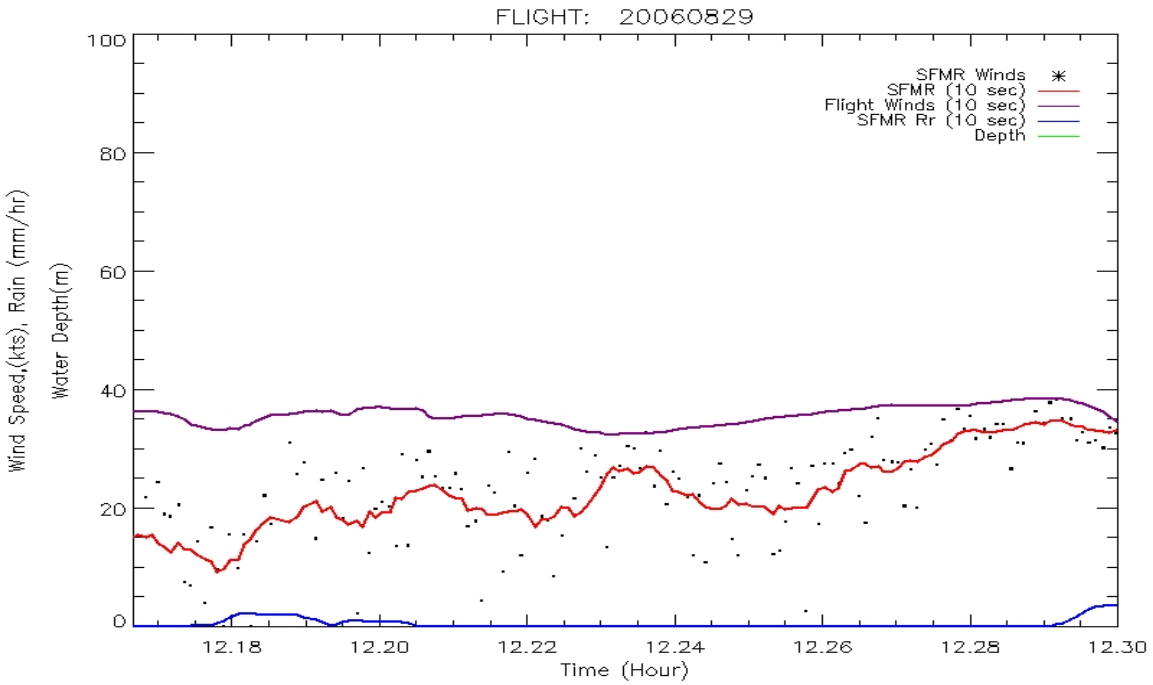

Figure 11: An anomaly in the SFMR wind retrieval is shown at approximately 12.23 hours on 29 August 2006.

2.1.2 Anomalies - 31 August 2006

The mission on 31 August 2006 occurred over deep water. During this mission, the observed anomalies in the SFMR wind speed retrievals occurred in the presence of precipitation. These features can be noted in Figure 12 at 15.30 and 15.33 hours, Figure 13 at 15.76 hours, Figure 14 at 16.04 hours and Figure 15 at 18.75 hours. Note that the response at 15.76 hours is a little less obvious. We believe the small dip in the winds is caused by the errors in the precipitation model.

Figure 16 shows the SFMR retrievals during a precipitation event and stronger wind speeds. In this case (i.e. stronger winds), the SFMR wind retrievals do not appear to be effected. We believe that for most cases where the winds are at hurricane force, this will be the situation or that the impact of precipitation will be less. Finally, once the precipitation model is corrected (i.e. 2nd year JHT effort), errors in the wind retrievals caused by precipitation will be removed or significantly reduced.

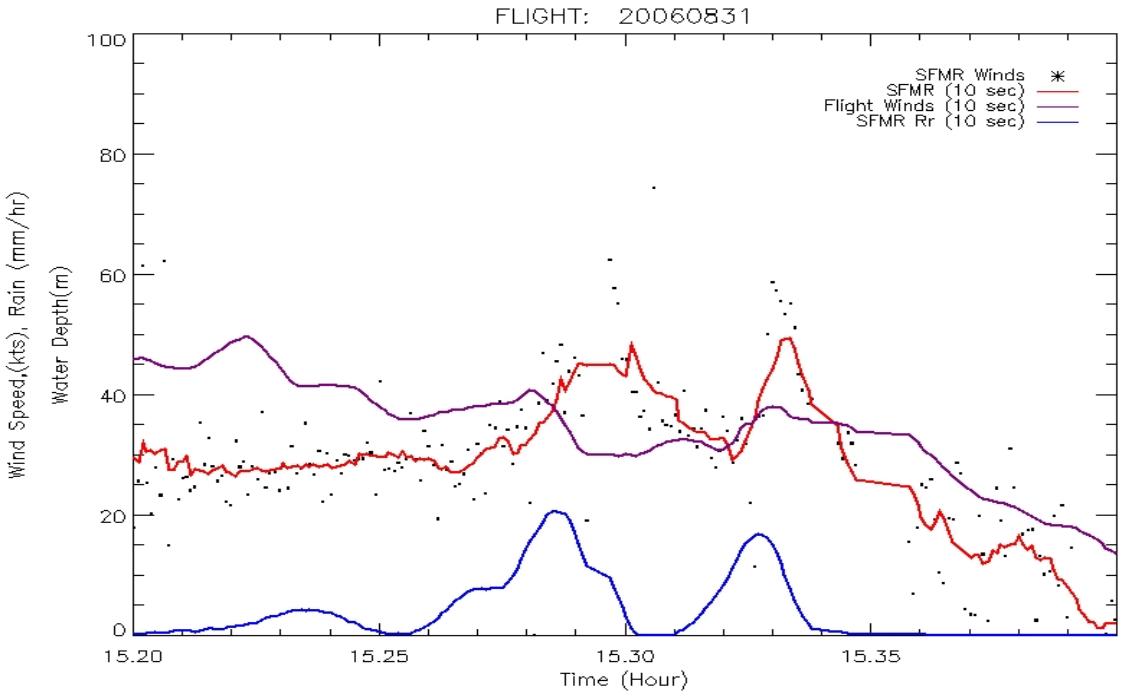

Figure 12: Anomalies in the SFMR wind retrieval are shown at approximately 15.3 and 15.33 on 31 August 2006.

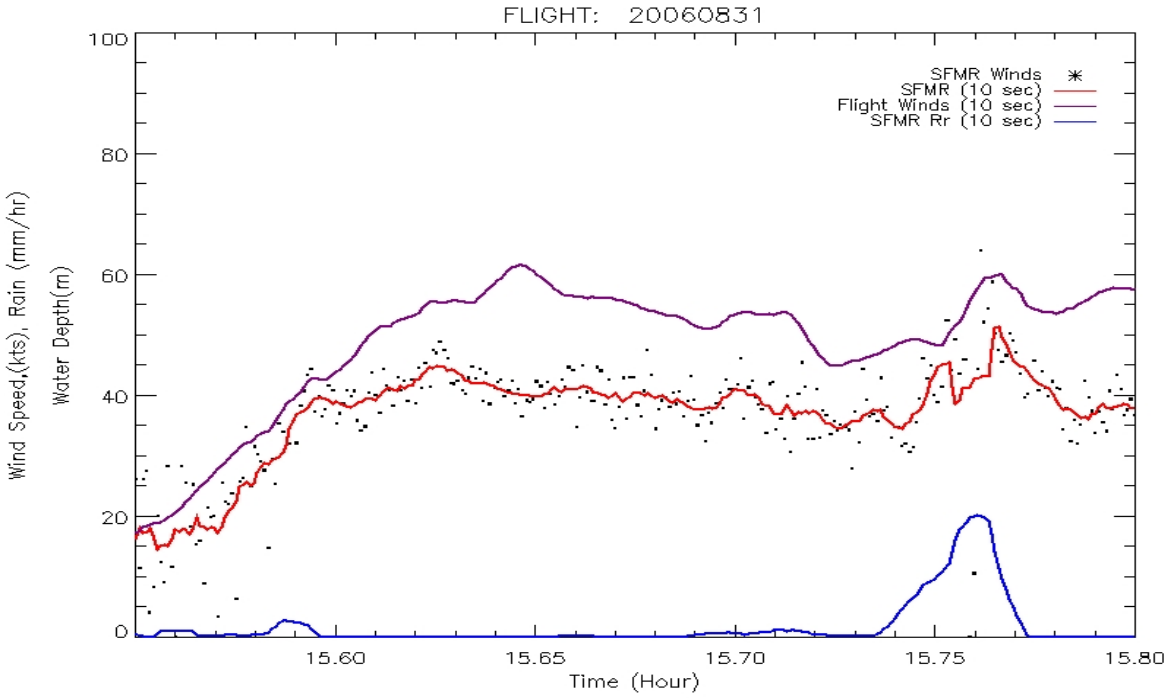

Figure 13: Anomaly in the SFMR wind retrieval is shown at approximately 15.76 hours on 31 August 2006.

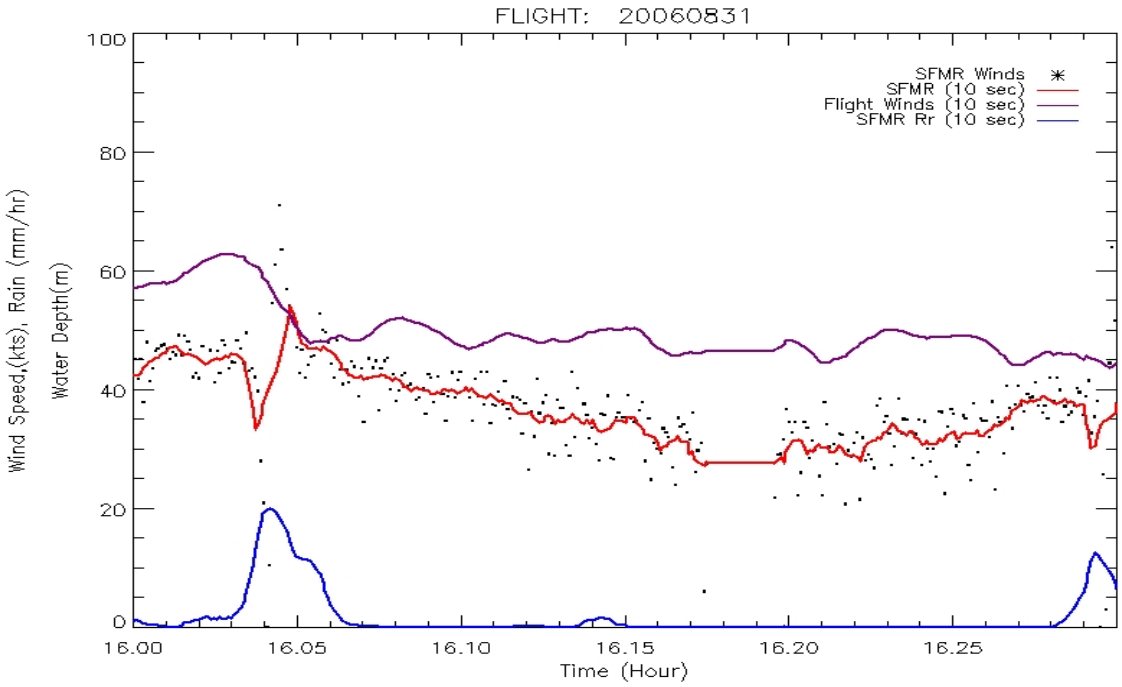

Figure 14: Anomalies in the SFMR wind retrieval are shown at approximately 16.05 and 16.3 hours on 31 August 2006.

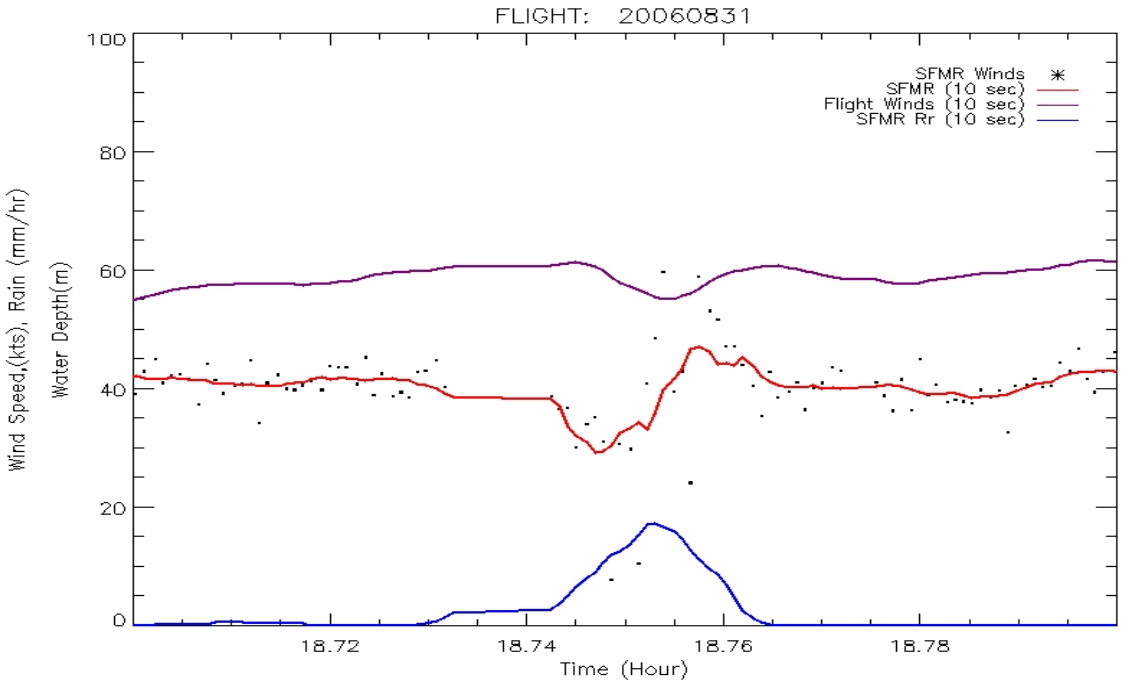

Figure 15: Anomaly in the SFMR wind retrieval is shown at approximately 18.75 hours on 31 August 2006.

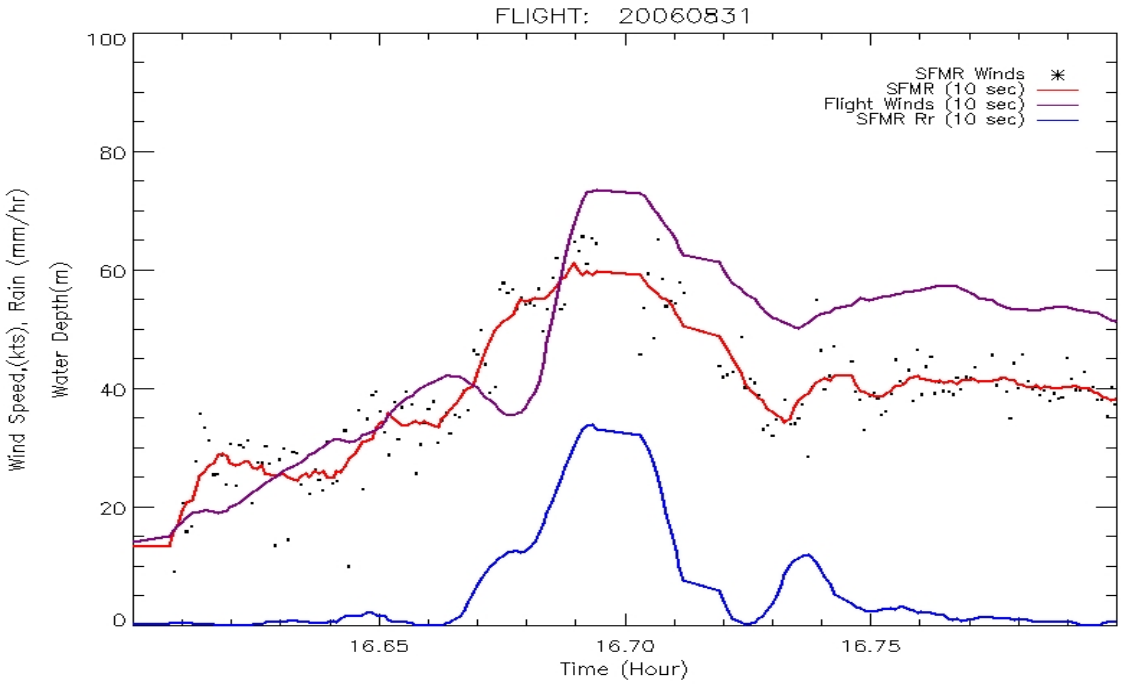

Figure 16: Example of SFMR wind retrievals unaffected by precipitation for stronger winds.

2.2 IWRAP – SFMR interference

During some of the 2006 hurricane missions, the IWRAP C-band transceiver was operated. During these missions, its lowest frequency channel transmitted at 4.985 GHz. When transmitting at this frequency, interference was noted in the lower frequency channel of the AOC SFMR (4.74 GHz). Because IWRAP operates at 20 KHz pulse repetition frequency and because AOC SFMR uses a fixed blanking period, the AOC SFMR could not be blanked during IWRAP transmission. The blanking technique is used by the SFMR to avoid being affected by radio frequency interference (RFI) from local radar systems (i.e. the C-band Lower Fuselage Radar). By viewing its internal loads rather than antenna port (i.e. blanking) while the interfering radar is transmitting and for some time there after, the AOC SFMR prevents viewing any RFI.

Since the SFMR could not use a blanking technique with IWRAP, the lower two channels were not used in the retrieval process. Note that the second lowest AOC SFMR channel falls in the middle of the IWRAP frequency band. This allowed the SFMR to retrieve the surface winds without contamination from IWRAP, but it also increased the variance in the wind speed retrievals. The reason is two fold. First, by using only four channels rather than six, the number of samples used in the retrieval decreases by 33 percent. This effectively increases the noise in the retrieval process because fewer samples are used to reduce the normal random noise in the measurements. Second, and more important, is that the maximum frequency separation of the measurements is decreased by 0.83 GHz. As a result, the retrieval process becomes more sensitive to the measurement noise. Recall that the retrieval process is a coupled

problem where the wind and rain rate are solved for simultaneously. The rain signature is strongly frequency dependent. By reducing the frequency separation in the measurements, measurement noise can be mistaken for rain causing both a wind speed and rain rate error. Because the measurement noise is random, a bias does not occur, but the variance of the retrievals increases. We ran simulations to determine the amount that the standard deviation of the wind speed retrievals would increase with the lower two frequency channels disabled.

Figure 17 presents the results. The upper plot shows the standard deviation in the wind speed retrievals as a function of wind speed when only the upper four SFMR frequency channels are used (dashed line) and when all six channels are used (solid line). The lower plot shows the percent increase in the standard deviation as a function of wind speed. These results are averaged over all rain rates because we found that there was no significant dependence on rain rate. As can be seen, operating with only the four upper channels results in about a 75 percent increase in the standard deviation in the wind speed retrievals. When the winds exceed storm force, the resultant standard deviation is less than 2 knots. Although this meets the original requirement for the SFMR, this additional error can be prevented for the 2007 hurricane season.

Working with UMass and NOAA, a series of measurements were acquired during the Winter 2007 Ocean Winds Experiment. Using a RF synthesizer, the IWRAP C-band transceiver was stepped through a series of frequencies from 4.7 GHz to 5.2 GHz in 50 MHz steps, dwelling for approximately 1 minute at each frequency, while the AOC SFMR collected its Tb measurements. All other IWRAP internal local oscillators were powered off. The Tb measurements were then analyzed when RFI was presented.

Figure 18 plots the AOC SFMR 4.74 GHz Tb measurements and the IWRAP frequency versus time. For frequencies below 5 GHz, RFI can be seen. To see the finer details, the mean Tb value for each IWRAP frequency interval was determined and subtracted from the Tb values. Figure 19 plots this difference. This procedure was repeated for the other five AOC SFMR frequency channels. Figure 20 through Figure 29 show the results. Note that the spikes seen at approximately 18.7, 18.75 and 18.977 hours are present in all six channels and are related to the synthesizer switching frequencies. From these results, we concluded that by slightly shifting the IWRAP lower transmission frequency just above 5 GHz, the lower two AOC SFMR channels will not be contaminated. We will work with NOAA and UMass to implement this change prior to the 2007 hurricane season.

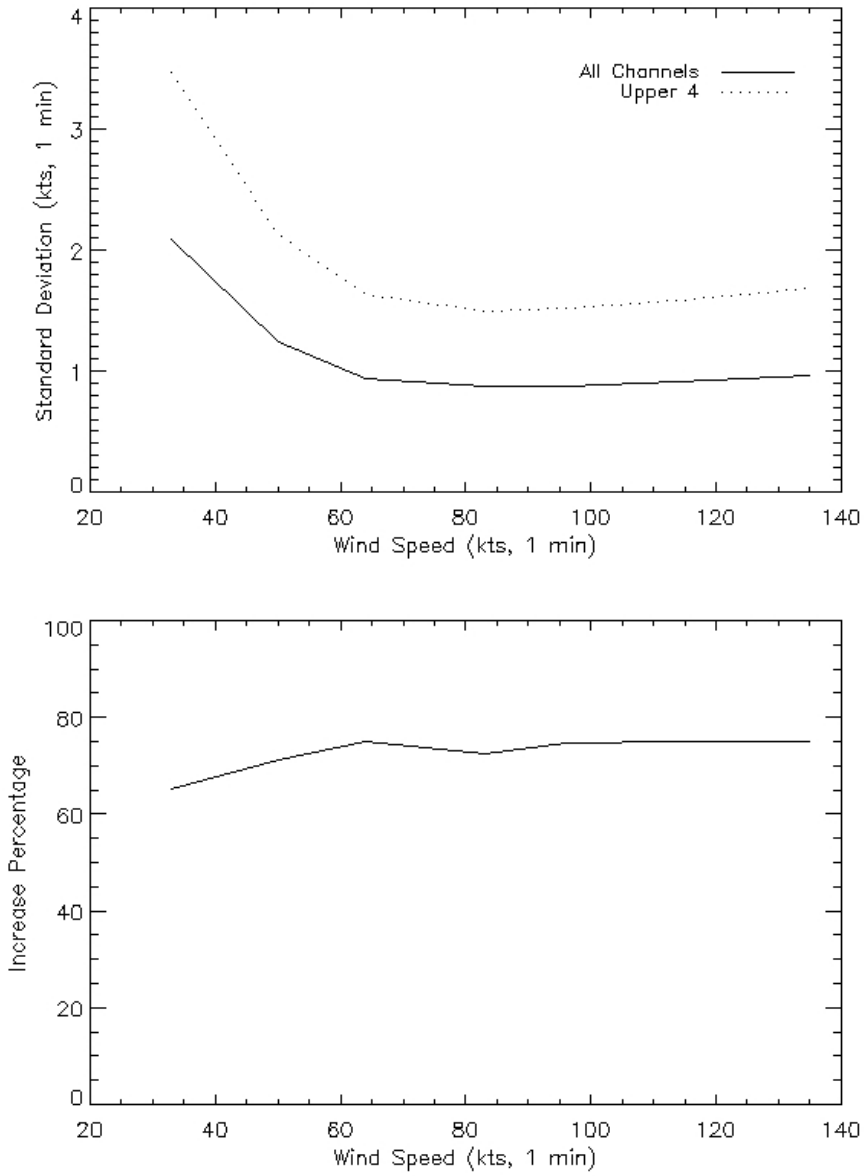

Figure 17: Effects on the SFMR wind speed retrievals caused by disabling lower two AOC SFMR frequency channels.

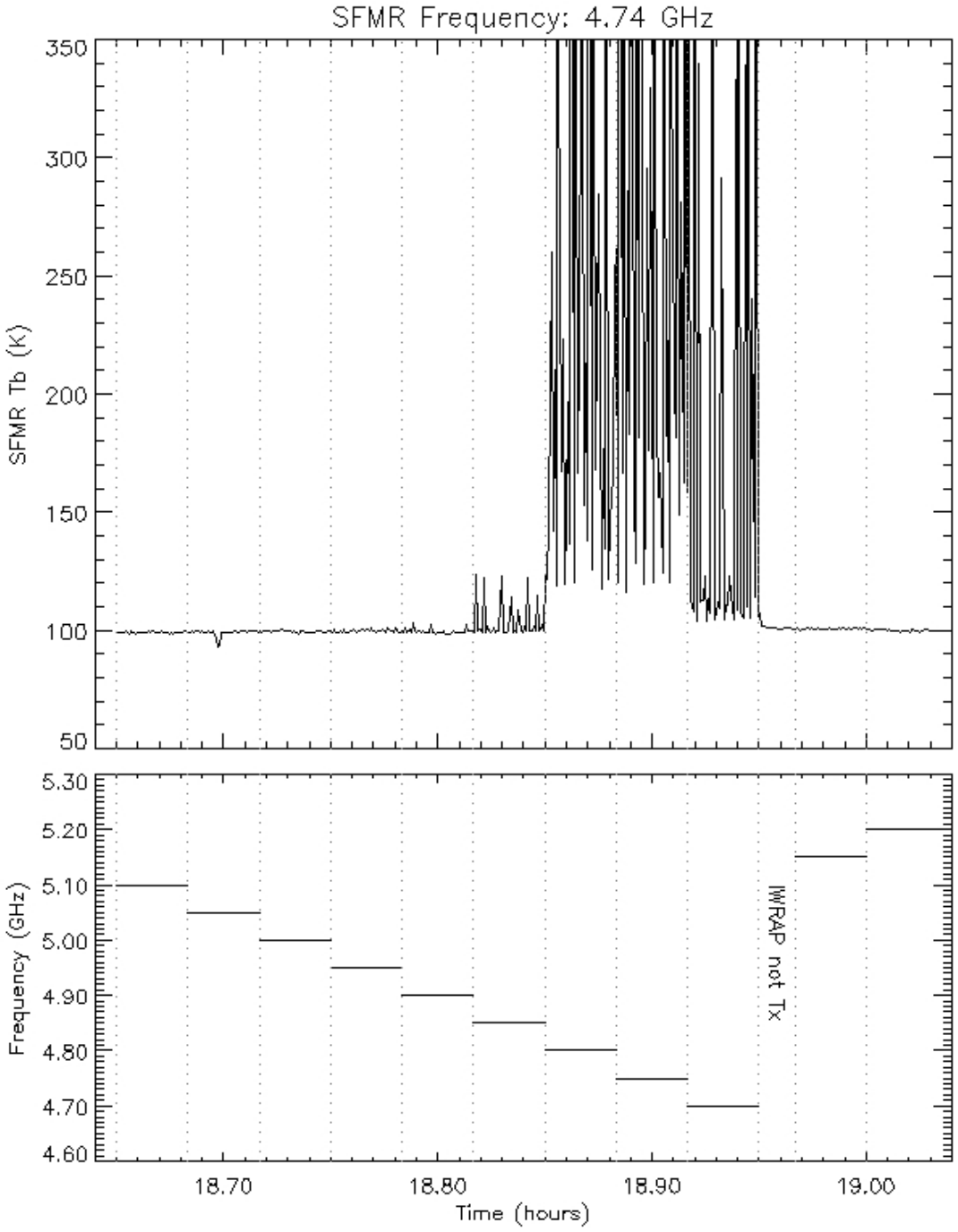

Figure 18: SFMR 4.74 GHz Tb measurements and IWRAP transmit frequency plotted versus time.

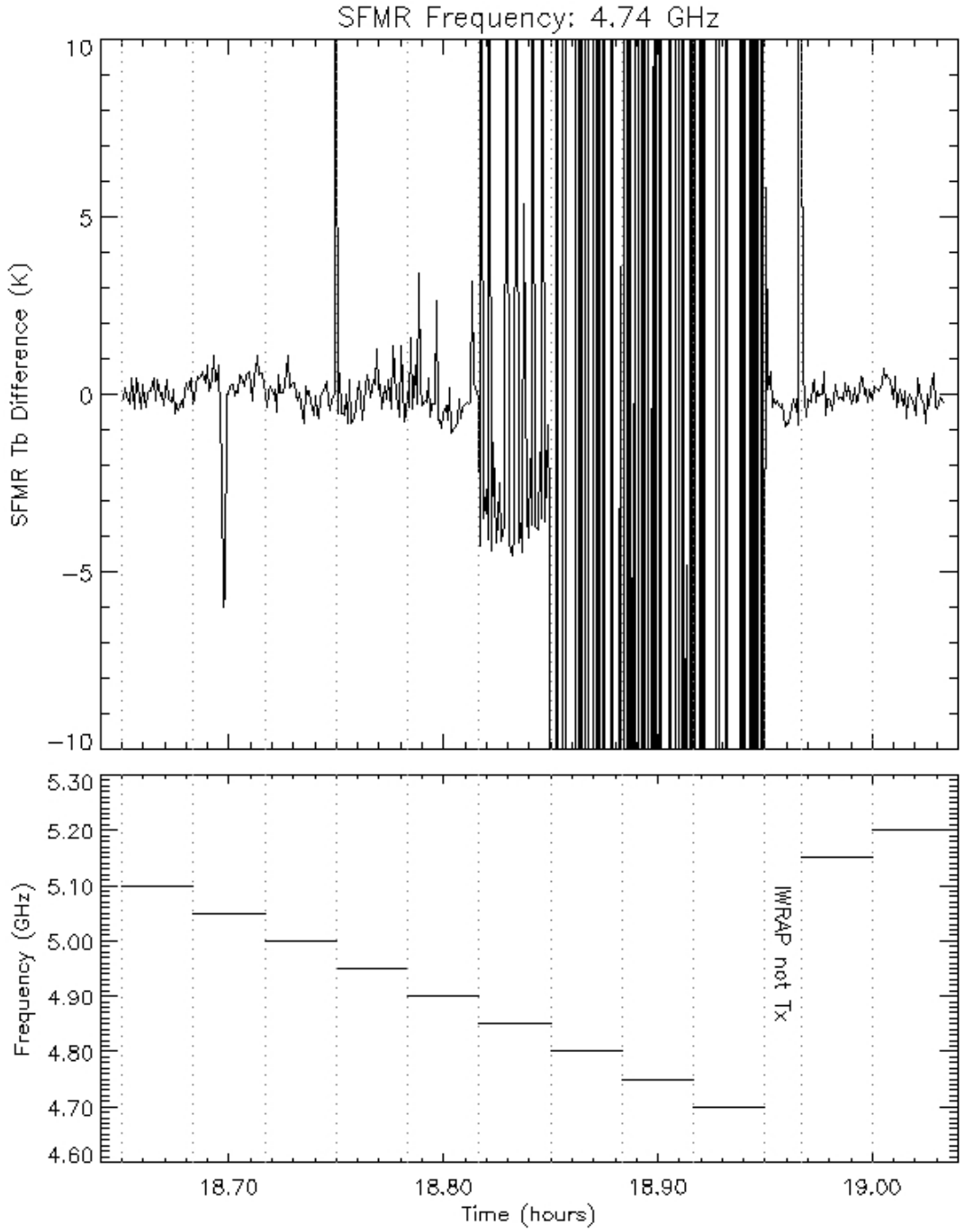

Figure 19: Difference in SFMR 4.74 GHz Tb measurements plotted versus time. Difference is calculated based on mean Tb for each IWRAP frequency interval.

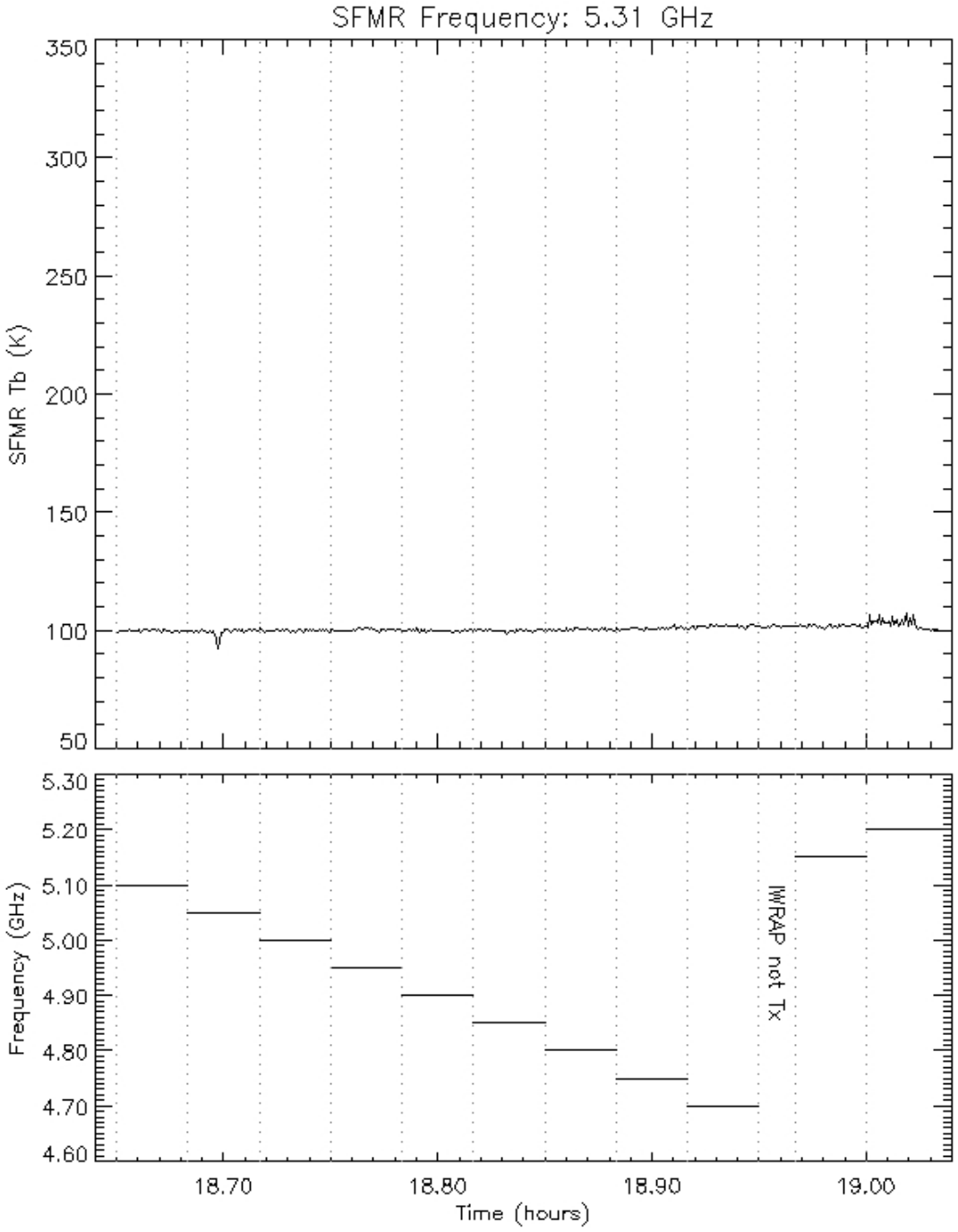

Figure 20: SFMR 5.31 GHz Tb measurements and IWRAP transmit frequency plotted versus time.

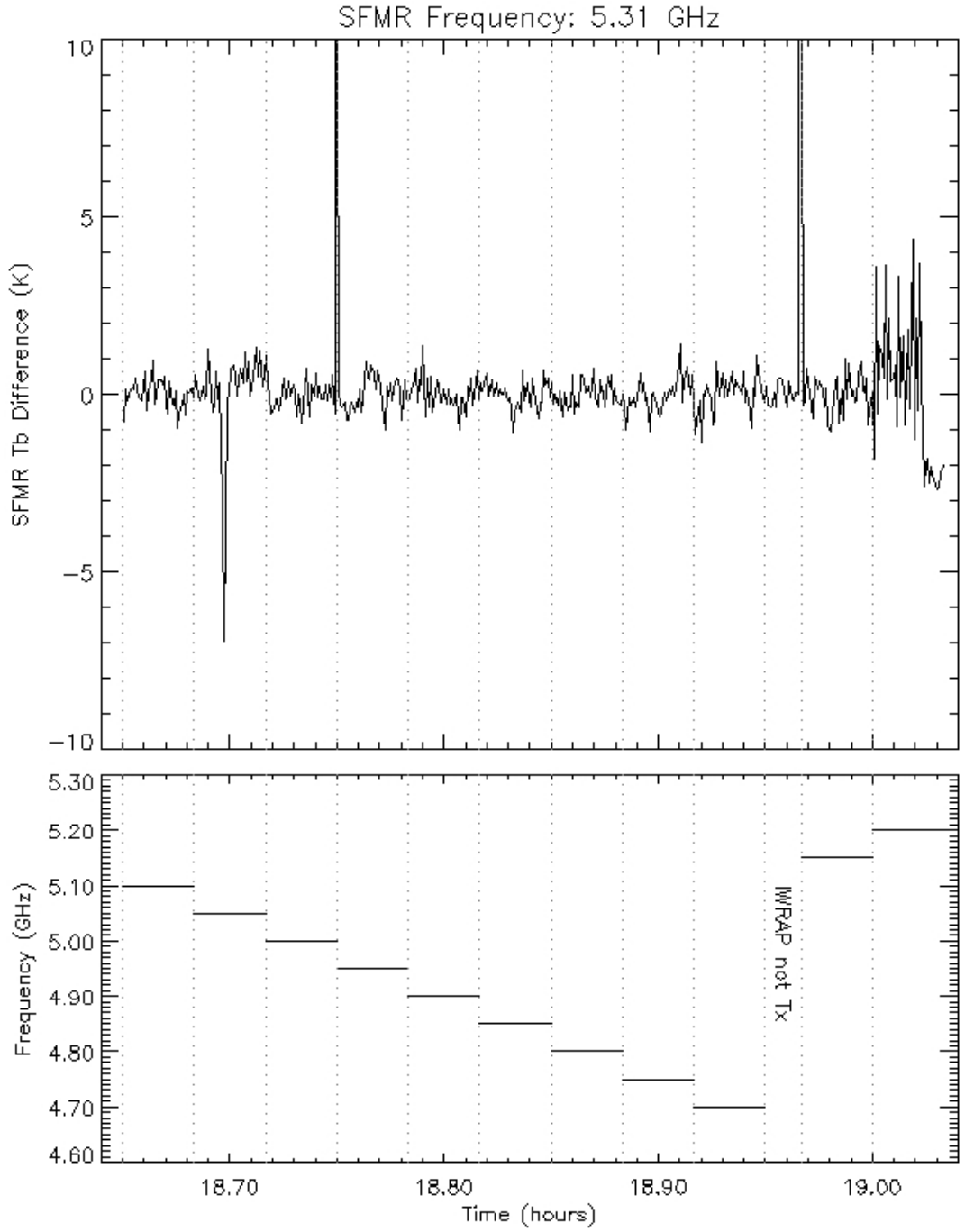

Figure 21: Difference in SFMR 5.31 GHz Tb measurements plotted versus time. Difference is calculated based on mean Tb for each IWRAP frequency interval.

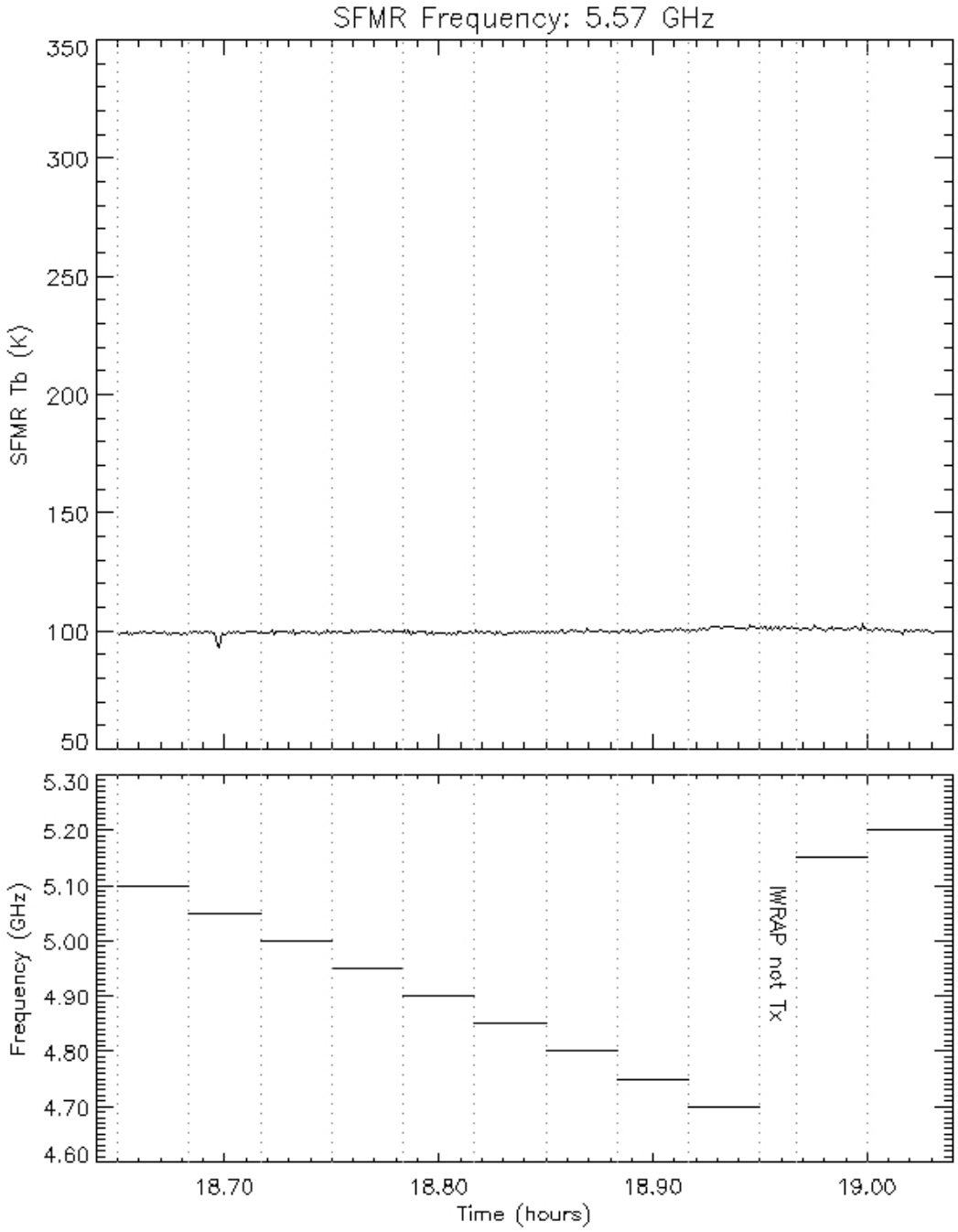

Figure 22: SFMR 5.57 GHz Tb measurements and IWRAP transmit frequency plotted versus time.

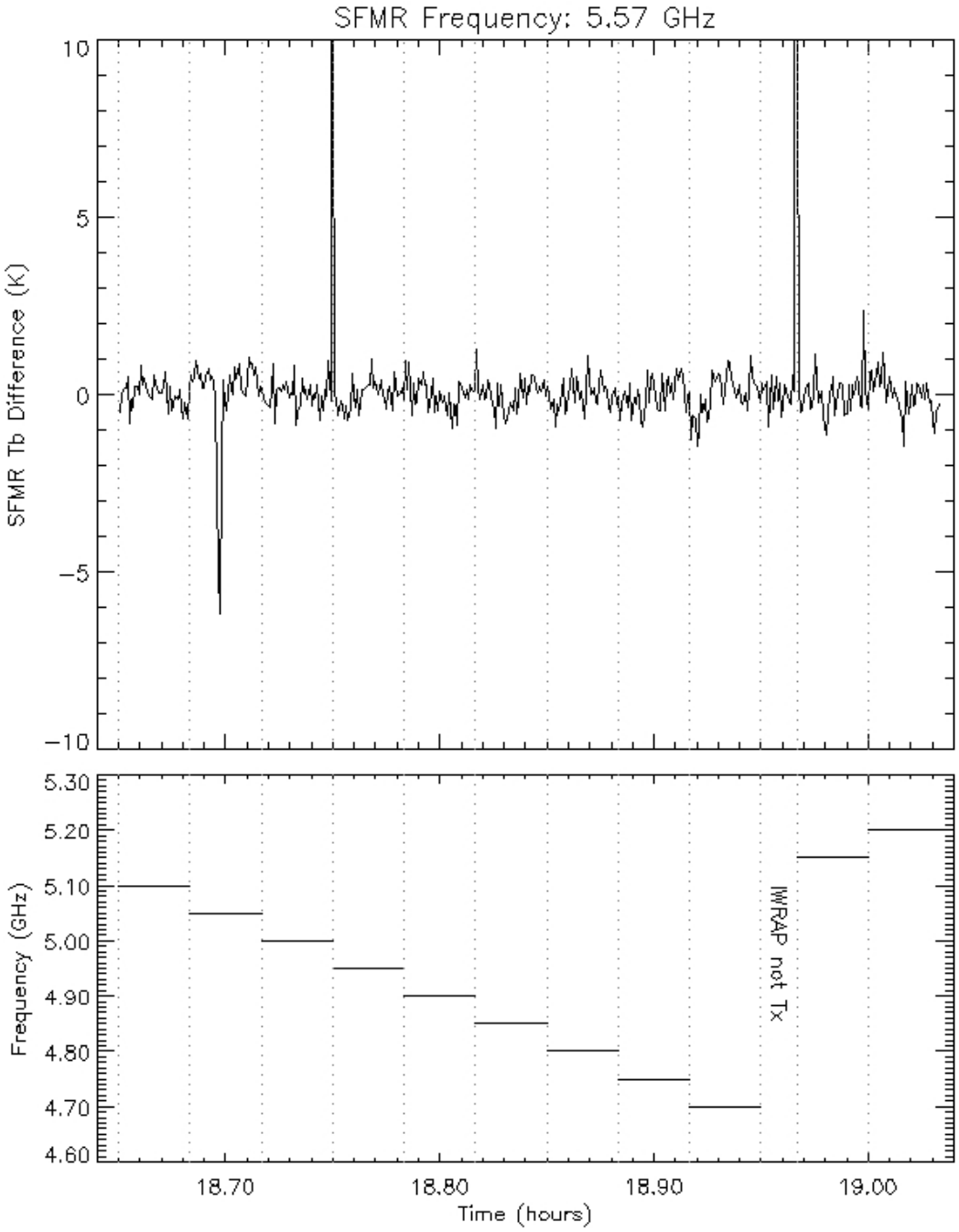

Figure 23: Difference in SFMR 5.57 GHz Tb measurements plotted versus time. Difference is calculated based on mean Tb for each IWRAP frequency interval.

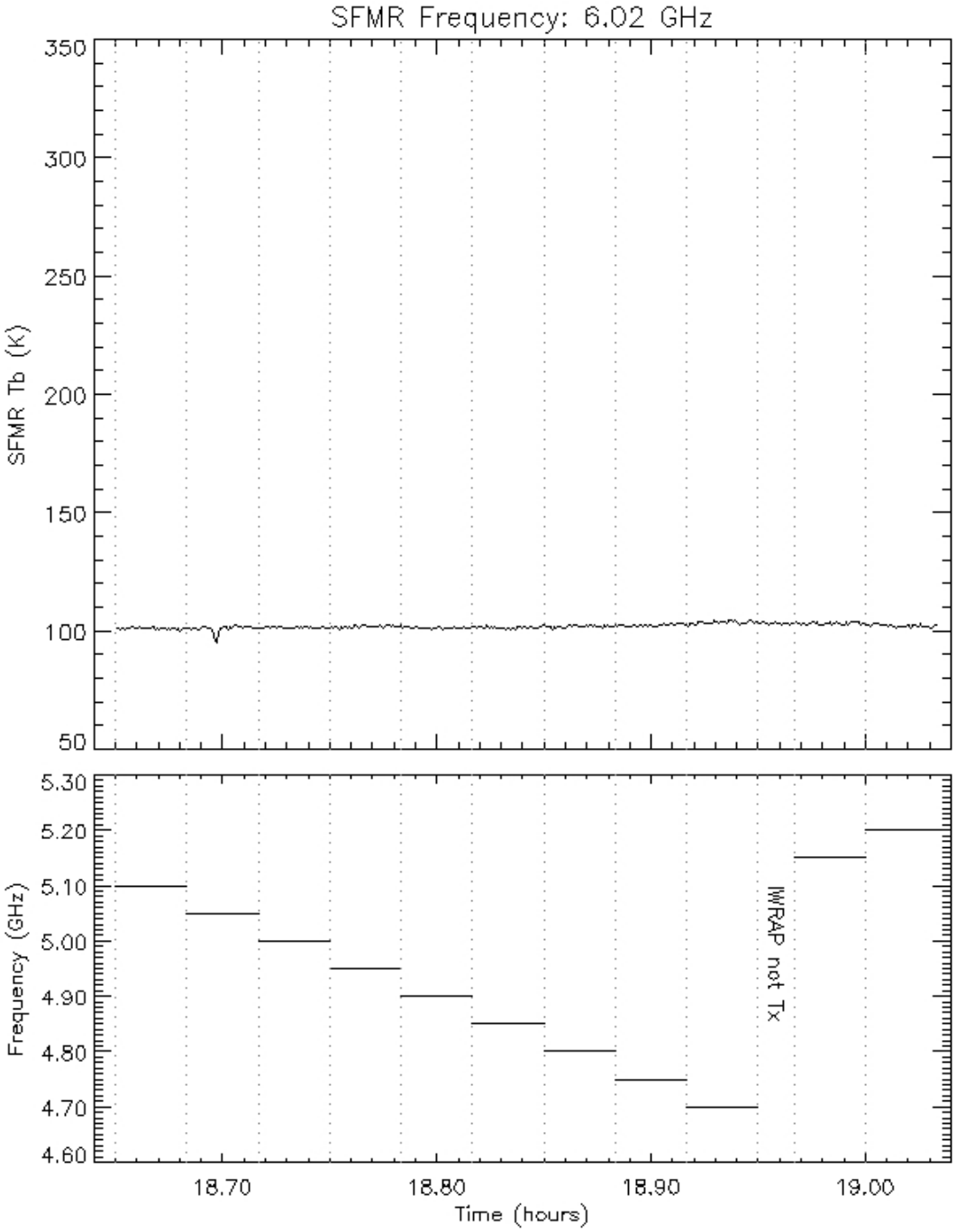

Figure 24: SFMR 6.02 GHz Tb measurements and IWRAP transmit frequency plotted versus time.

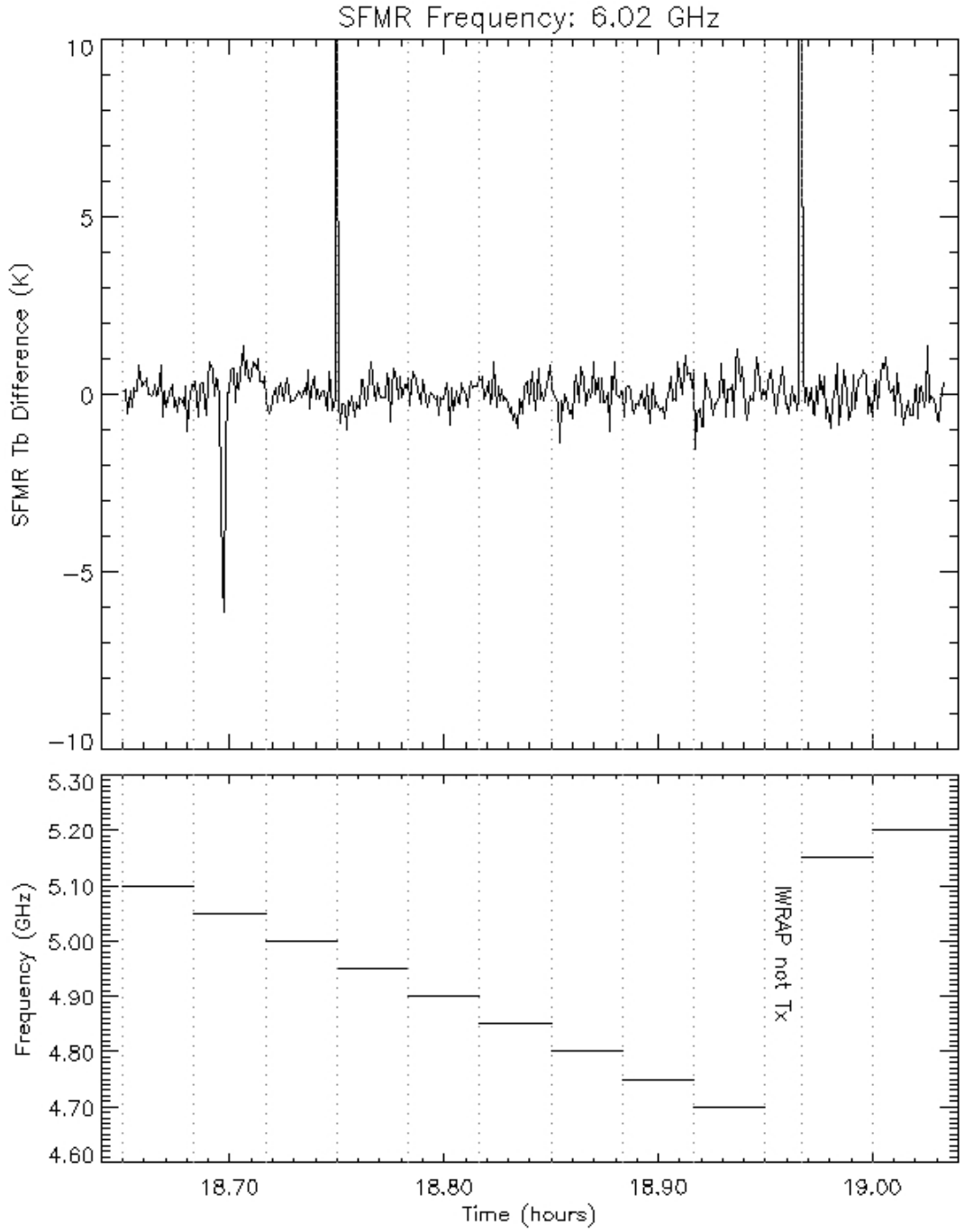

Figure 25: Difference in SFMR 6.02 GHz Tb measurements plotted versus time. Difference is calculated based on mean Tb for each IWRAP frequency interval.

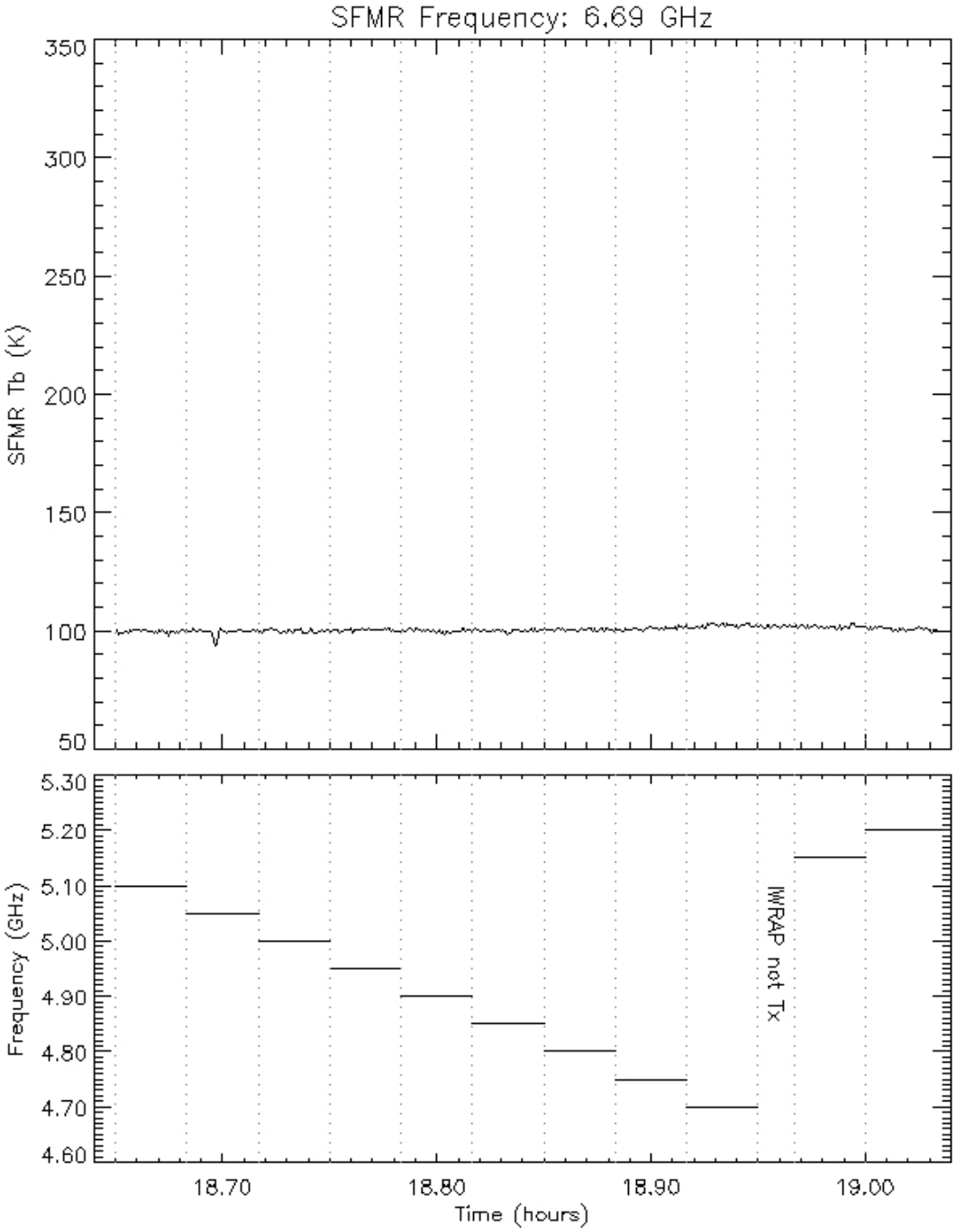

Figure 26: SFMR 6.69 GHz Tb measurements and IWRAP transmit frequency plotted versus time.

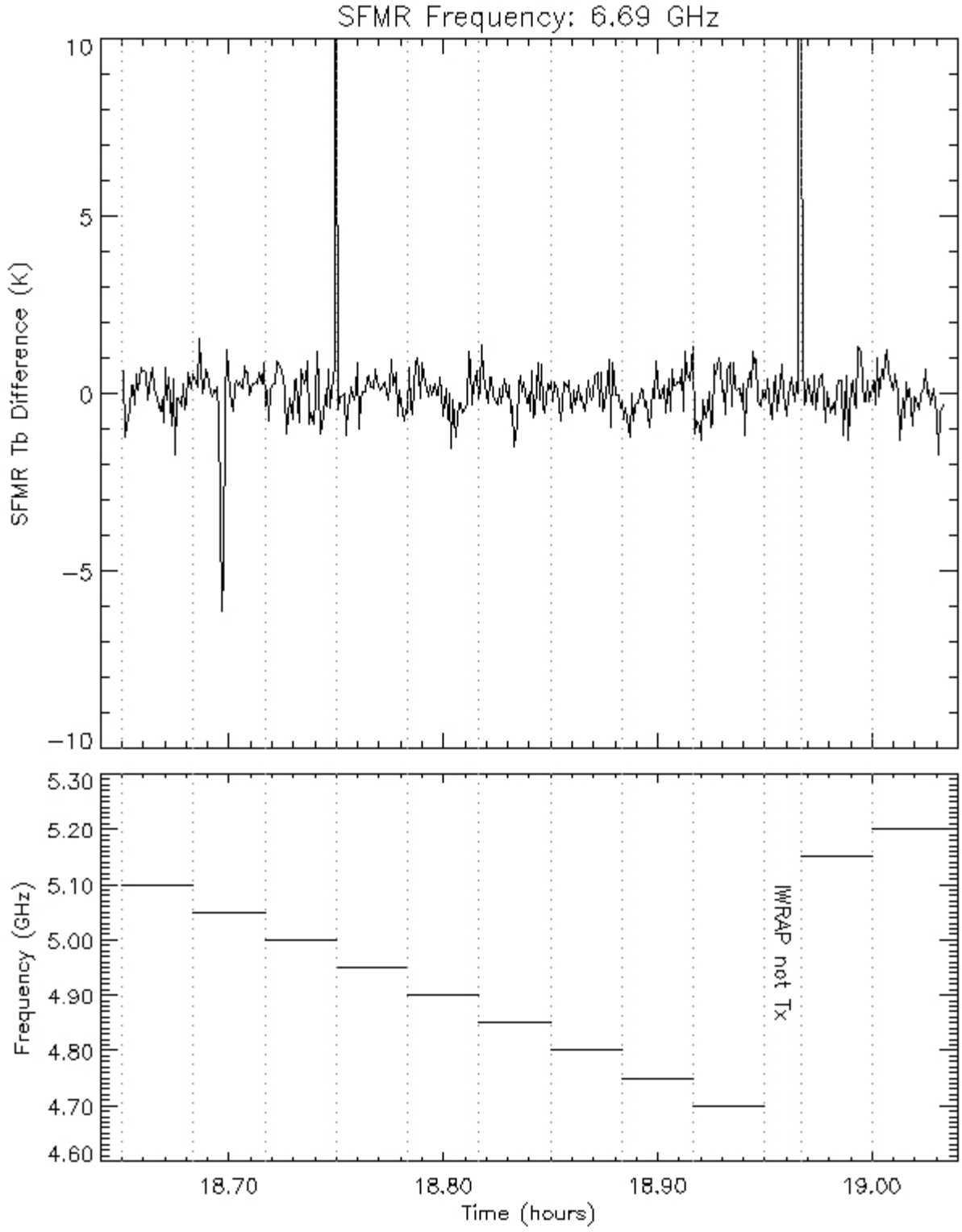

Figure 27: Difference in SFMR 6.69 GHz Tb measurements plotted versus time. Difference is calculated based on mean Tb for each IWRAP frequency interval.

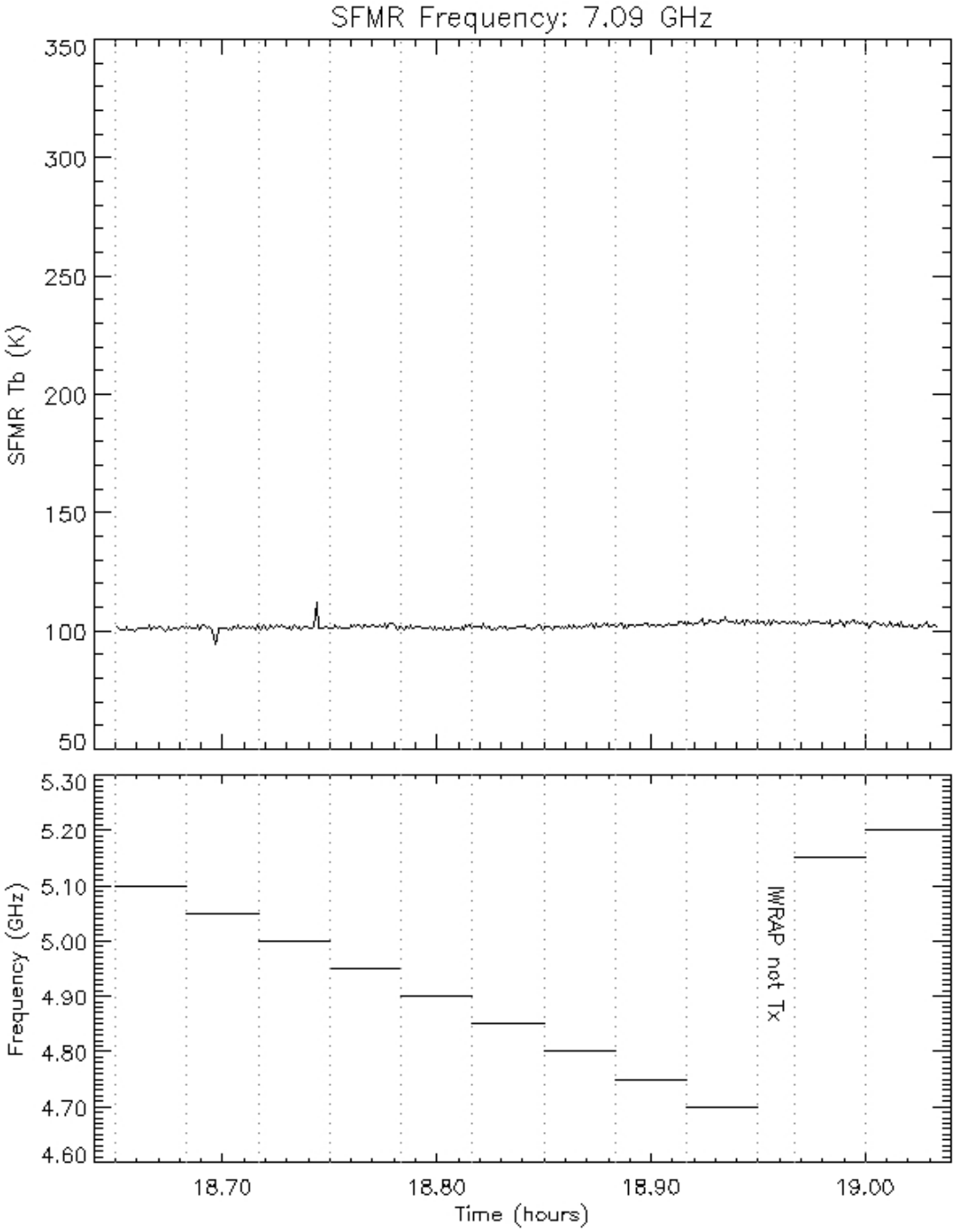

Figure 28: SFMR 7.09 GHz Tb measurements and IWRAP transmit frequency plotted versus time.

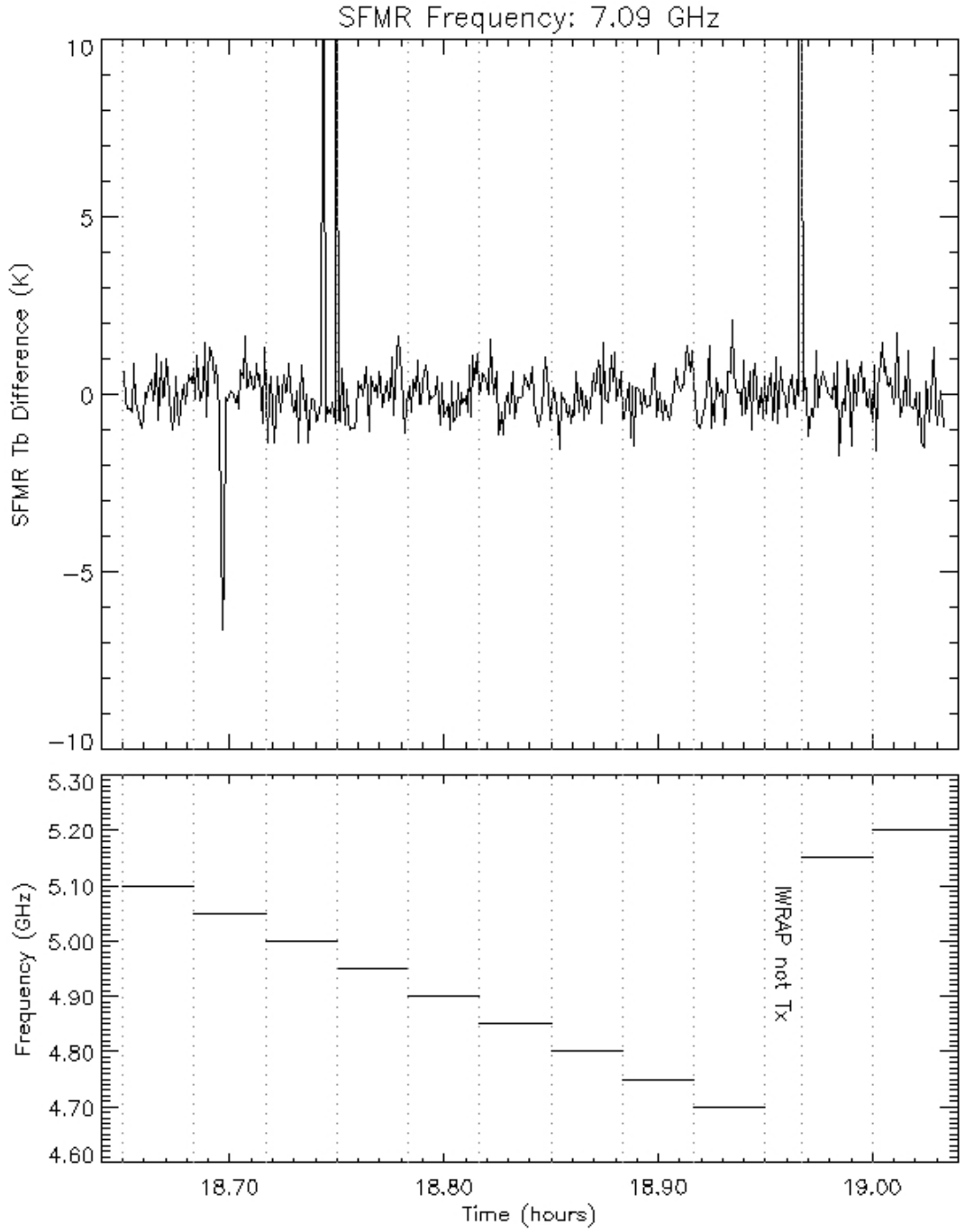

Figure 29: Difference in SFMR 7.09 GHz Tb measurements plotted versus time. Difference is calculated based on mean Tb for each IWRAP frequency interval.

2.3 Precipitation GMF

One of the primary objectives of the 2nd year JHT effort is to improve the precipitation GMF used by the SFMR retrieval process. As noted previously, errors in this GMF result in both wind speed and rain rate errors. In our 1st year annual report, we discussed how errors in the various tuning parameters within the rain GMF can cause both wind speed and rain rate errors. Therefore it is critical to address the deficiencies in this model.

To do so, we proposed to use coincident precipitation observations collected with the IWRAP. This instrument measures the Doppler-reflectivity profiles at C and Ku-band and at different incidence angles while it conically scans. It has been flown alongside the AOC SFMR on the NOAA WP-3D aircraft during the 2005 and 2006 seasons. From its dual-wavelength reflectivity profiles, the attenuation suffered at Ku-band along the path can be measured. From these attenuation profiles the precipitation can be retrieved.

To verify this approach, we have analyzed two independent data sets. First IWRAP measurements obtained in 2003 during flights through Hurricane Isabel were collocated with the UMass SFMR rain rate estimates. The Ku-band specific attenuation was estimated using differential attenuation techniques. Figure 30 (a) plots the Ku-band specific attenuation derived from IWRAP measurements plotted versus the SFMR derived rain rate estimates. Overlaid is a model function that predicts the specific attenuation as a function of rain rate. As this figure shows, the SFMR rain rates under predict the “true” rain rate, assuming the specific attenuation models are correct. Scaling the SFMR rain rates by a factor of 2.5 and adding a small offset of approximately 5 mm/hr, the measurements are then in agreement with the models (see Figure 30 (b)).

Using the same specific attenuation models, we derived rain rate estimates from the IWRAP measurements collected during a flight through Hurricane Rita on 22 September 2005. We then collocated these estimates with the AOC rain rate estimates. The collocated AOC and IWRAP rain rate estimates were divided into 2.5 mm/hr bins and averaged. Figure 31 plots the results. Once again, we found the SFMR rate rates to be under estimated by a factor of 2.5. That is, the slope of the linear regression between the SFMR and IWRAP rain rate estimates is 0.4. These independent results agree with those obtained from the 2003 data. Further, the correlation between these two sets of retrievals (IWRAP and the SFMR) is 98 percent. This verifies that this approach is robust and consistent. We are currently processing the remainder of the 2005 IWRAP data. From which the SFMR rain GMF can be improved.

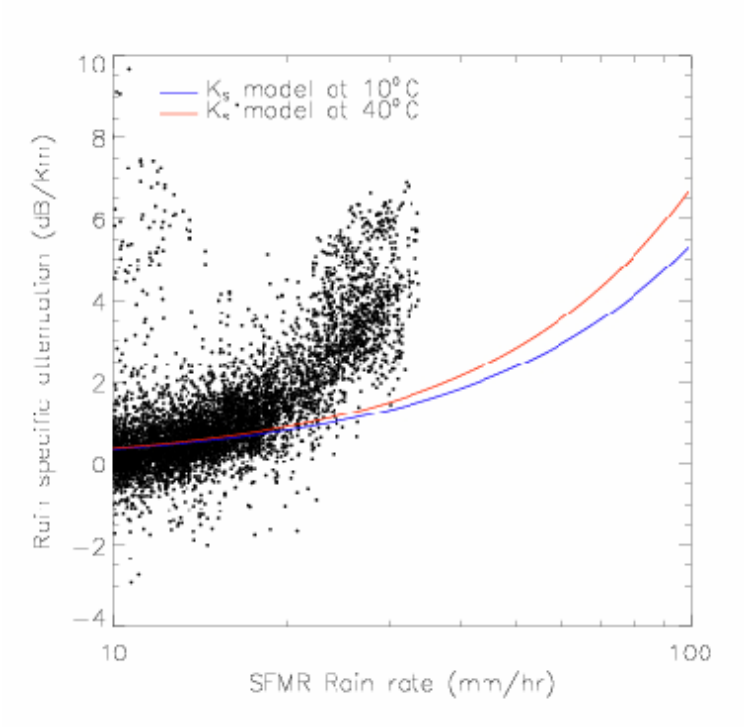

(a)

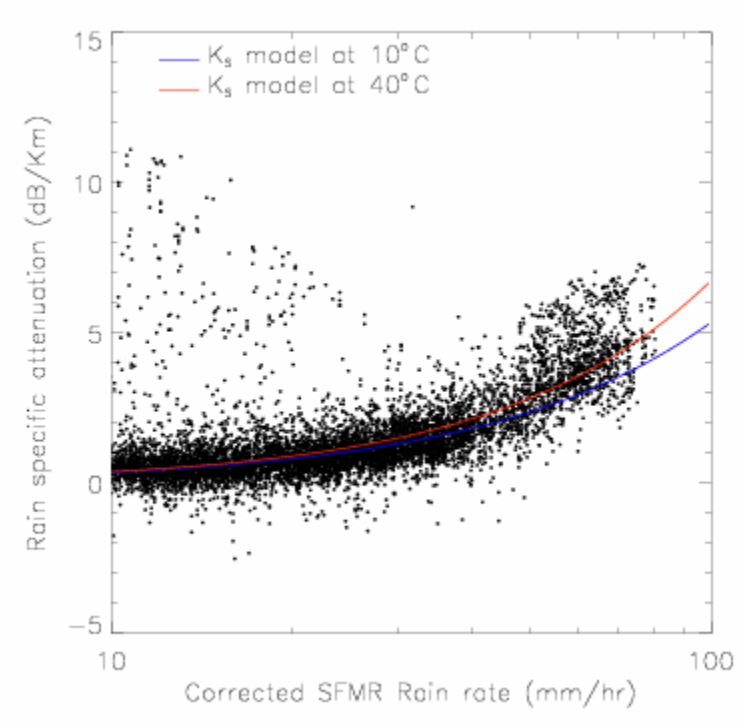

(b)

Figure 30: IWRAP derived specific attenuation plotted versus the UMass SFMR rain rate estimates (a) and corrected rain rate estimates (b). These observations collected through a series of flights through Hurricane Isabel in 2003.

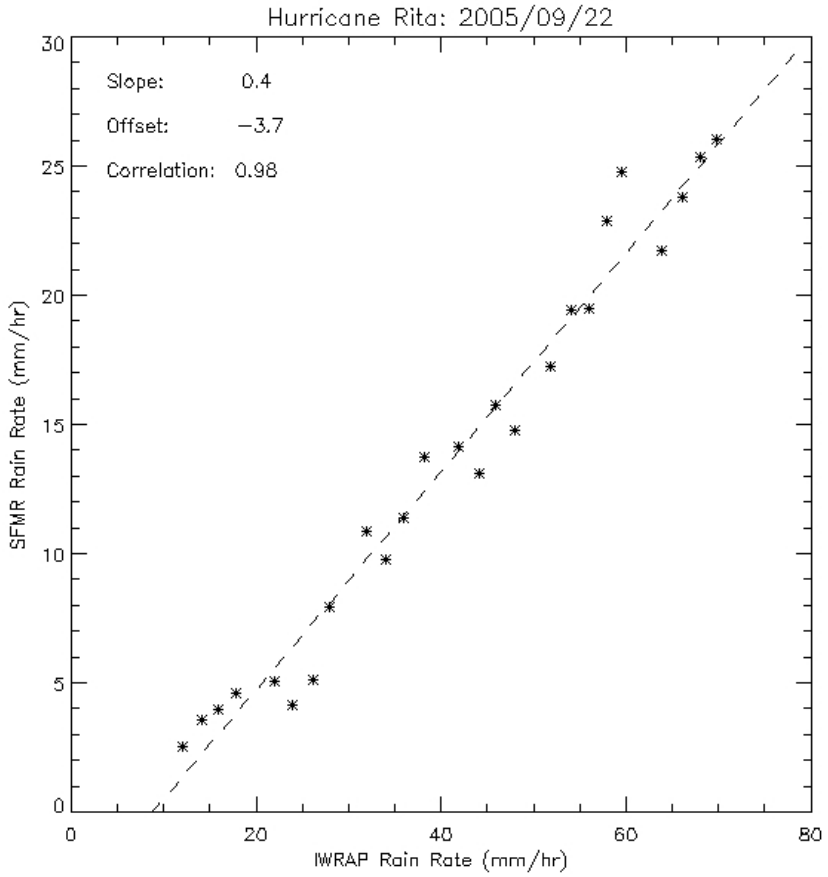

Figure 31: SFMR bin averaged rain rate estimates are plotted versus IWRAP rain rate estimates. The dashed line is a linear regression with the slope, offset and correlation coeffients given in the legend.

3 Second Year Work to be Completed

Over the next two months, we will complete the processing of the 2005 IWRAP rain retrievals. These data will be collocated with the AOC SFMR rain retrievals. A subset of this collocated data set will be used to refine the SFMR rain GMF. The SFMR retrieval process will be updated to use the new GMF and retrievals from all 2005 data will be derived again. The new rain retrievals will be validated against the IWRAP rain retrievals. Once validated, the wind retrievals will be compared against in-situ wind measurements from collocated GPS dropsonde winds. The 2006 SFMR retrievals will also be derived again. Specifically, cases where anomalies believed to be caused by deficiencies in the rain GMF will be analyzed. Further refinements to the new rain GMF will be made as required. A report on the new GMF will be compiled for review in May. We will work closely with Alan Goldstein to ensure AOC is kept abreast of our progress and that any recommended changes can be implemented by AOC if approved by the JHT review panel. Bi-monthly conference calls will begin following the annual IHC meeting. These conference calls will include representatives from AOC, HRD, ORA (now called STAR) and RSS.

In parallel, we will also be working on updating the land flag database to include areas where shallow bathymetry have caused anomalies in the SFMR retrievals; we will define specific flight patterns and procedures to further aid in determining affects of shallow bathymetry on the SFMR retrievals; we will update the SFMR retrieval process to better handle the noisy statistics of the brightness temperature measurements under rain free conditions; and we will work on implementing real-time algorithms to estimate advanced products such as hurricane radii and maximum sustained winds. The results of these efforts will also be compiled in report documents for review prior to the completion of the second year effort.